



Grado en Ingeniería en Tecnologías Industriales

Trabajo de Fin de Grado

**PRESSURE WAVES ANALYSIS FOR
INTERNAL COMBUSTION ENGINE
EFFICIENCY OPTIMIZATION**

Autor:

Álvaro Loureiro Orejas

Supervisor:

Jesper Schramm

Madrid

Agosto de 2020

AUTORIZACIÓN PARA LA DIGITALIZACIÓN, DEPÓSITO Y DIVULGACIÓN EN RED DE PROYECTOS FIN DE GRADO, FIN DE MÁSTER, TESINAS O MEMORIAS DE BACHILLERATO

1º. Declaración de la autoría y acreditación de la misma.

El autor D. _____

DECLARA ser el titular de los derechos de propiedad intelectual de la obra:

_____,
que ésta es una obra original, y que ostenta la condición de autor en el sentido que otorga la Ley de Propiedad Intelectual.

2º. Objeto y fines de la cesión.

Con el fin de dar la máxima difusión a la obra citada a través del Repositorio institucional de la Universidad, el autor **CEDE** a la Universidad Pontificia Comillas, de forma gratuita y no exclusiva, por el máximo plazo legal y con ámbito universal, los derechos de digitalización, de archivo, de reproducción, de distribución y de comunicación pública, incluido el derecho de puesta a disposición electrónica, tal y como se describen en la Ley de Propiedad Intelectual. El derecho de transformación se cede a los únicos efectos de lo dispuesto en la letra a) del apartado siguiente.

3º. Condiciones de la cesión y acceso

Sin perjuicio de la titularidad de la obra, que sigue correspondiendo a su autor, la cesión de derechos contemplada en esta licencia habilita para:

- a) Transformarla con el fin de adaptarla a cualquier tecnología que permita incorporarla a internet y hacerla accesible; incorporar metadatos para realizar el registro de la obra e incorporar “marcas de agua” o cualquier otro sistema de seguridad o de protección.
- b) Reproducirla en un soporte digital para su incorporación a una base de datos electrónica, incluyendo el derecho de reproducir y almacenar la obra en servidores, a los efectos de garantizar su seguridad, conservación y preservar el formato.
- c) Comunicarla, por defecto, a través de un archivo institucional abierto, accesible de modo libre y gratuito a través de internet.
- d) Cualquier otra forma de acceso (restringido, embargado, cerrado) deberá solicitarse expresamente y obedecer a causas justificadas.
- e) Asignar por defecto a estos trabajos una licencia Creative Commons.
- f) Asignar por defecto a estos trabajos un HANDLE (URL *persistente*).

4º. Derechos del autor.

El autor, en tanto que titular de una obra tiene derecho a:

- a) Que la Universidad identifique claramente su nombre como autor de la misma
- b) Comunicar y dar publicidad a la obra en la versión que ceda y en otras posteriores a través de cualquier medio.
- c) Solicitar la retirada de la obra del repositorio por causa justificada.
- d) Recibir notificación fehaciente de cualquier reclamación que puedan formular terceras personas en relación con la obra y, en particular, de reclamaciones relativas a los derechos de propiedad intelectual sobre ella.

5º. Deberes del autor.

El autor se compromete a:

- a) Garantizar que el compromiso que adquiere mediante el presente escrito no infringe ningún derecho de terceros, ya sean de propiedad industrial, intelectual o cualquier otro.
- b) Garantizar que el contenido de las obras no atenta contra los derechos al honor, a la intimidad y a la imagen de terceros.
- c) Asumir toda reclamación o responsabilidad, incluyendo las indemnizaciones por daños, que pudieran ejercitarse contra la Universidad por terceros que vieran infringidos sus derechos e

intereses a causa de la cesión.

- d) Asumir la responsabilidad en el caso de que las instituciones fueran condenadas por infracción de derechos derivada de las obras objeto de la cesión.

6º. Fines y funcionamiento del Repositorio Institucional.

La obra se pondrá a disposición de los usuarios para que hagan de ella un uso justo y respetuoso con los derechos del autor, según lo permitido por la legislación aplicable, y con fines de estudio, investigación, o cualquier otro fin lícito. Con dicha finalidad, la Universidad asume los siguientes deberes y se reserva las siguientes facultades:

- La Universidad informará a los usuarios del archivo sobre los usos permitidos, y no garantiza ni asume responsabilidad alguna por otras formas en que los usuarios hagan un uso posterior de las obras no conforme con la legislación vigente. El uso posterior, más allá de la copia privada, requerirá que se cite la fuente y se reconozca la autoría, que no se obtenga beneficio comercial, y que no se realicen obras derivadas.
- La Universidad no revisará el contenido de las obras, que en todo caso permanecerá bajo la responsabilidad exclusiva del autor y no estará obligada a ejercitar acciones legales en nombre del autor en el supuesto de infracciones a derechos de propiedad intelectual derivados del depósito y archivo de las obras. El autor renuncia a cualquier reclamación frente a la Universidad por las formas no ajustadas a la legislación vigente en que los usuarios hagan uso de las obras.
- La Universidad adoptará las medidas necesarias para la preservación de la obra en un futuro.
- La Universidad se reserva la facultad de retirar la obra, previa notificación al autor, en supuestos suficientemente justificados, o en caso de reclamaciones de terceros.

Madrid, a 17 de Agosto de 2020

ACEPTA

Fdo. *Alvaro Loureiro*

Motivos para solicitar el acceso restringido, cerrado o embargado del trabajo en el Repositorio Institucional:

--

Declaro, bajo mi responsabilidad, que el Proyecto presentado con el título
‘Pressure waves analysis for internal combustion engine optimization’
en la ETS de Ingeniería - ICAI de la Universidad Pontificia Comillas en el
curso académico 2019-2020 es de mi autoría, original e inédito y
no ha sido presentado con anterioridad a otros efectos. El Proyecto no es plagio de otro,
ni total ni parcialmente y la información que ha sido tomada
de otros documentos está debidamente referenciada.

Fdo.: *Alvaro Loureiro* Fecha: 21/08/2020

Autorizada la entrega del proyecto

EL DIRECTOR DEL PROYECTO

Fdo.: *Jesper Schramm* Fecha: 21/08/2020



Grado en Ingeniería en Tecnologías Industriales

Trabajo de Fin de Grado

**PRESSURE WAVES ANALYSIS FOR
INTERNAL COMBUSTION ENGINE
EFFICIENCY OPTIMIZATION**

Autor:

Álvaro Loureiro Orejas

Supervisor:

Jesper Schramm

Madrid

Agosto de 2020

ANÁLISIS DE LAS ONDAS DE PRESIÓN PARA LA OPTIMIZACIÓN DEL MOTOR DE COMBUSTIÓN INTERNA

Autor: Loureiro Orejas, Álvaro.

Director: Jesper Schramm.

Entidad Colaboradora: Danmarks Tekniske Universitet.

RESUMEN DEL PROYECTO

1.- Introducción

Los motores de combustión interna de cuatro tiempos extraen energía de la combustión de aire y combustible, pero solo la fase de explosión genera energía. El resto de las fases preparan el motor para la fase de explosión: la admisión llena el cilindro con aire y combustible, la fase de compresión eleva la presión del cilindro antes de que la fase de explosión extraiga la potencia y la fase de escape vacía el cilindro de los gases resultantes de la combustión, preparando el motor para otro ciclo.

La potencia obtenida en el cigüeñal depende de la cantidad de combustible quemado, que es constante debido a la relación aire-combustible. Sin embargo, si aumenta la cantidad de aire introducido en el cilindro en la fase de admisión, se puede quemar más combustible y con ello se aumentaría la potencia en el cigüeñal.

Para lograr esto último, los fabricantes han diseñado varios mecanismos para intentar mejorar sus motores de combustión interna. Existen distintos mecanismos que conducen a una mejora en el intercambio de aire y el llenado del cilindro, siendo dos de los más importantes la distribución variable de válvulas y el colector de admisión de longitud variable. Los sistemas de sincronización variable de válvulas superan en rendimiento a aquellos con válvulas estándar debido a la capacidad de cambiar la duración y la distribución de las válvulas de admisión y escape. Cuando el motor funciona a velocidades altas, el motor requiere tiempos de apertura más largos que cuando funciona a velocidades más bajas. Los sistemas de distribución variable de válvulas pueden cambiar a una determinada velocidad del motor de una configuración a otra, mejorando el rendimiento del motor.

Los colectores de admisión de longitud variable aprovechan las ondas de presión producidas por el motor para elevar la presión del puerto de admisión cuando la válvula de admisión está en descenso. La particularidad de este sistema es que varía su longitud en función del régimen del motor para optimizar el rendimiento y conseguir introducir más aire en el cilindro. Mientras que los conductos de admisión de longitud constante pueden ser perjudiciales a ciertas velocidades del motor, los conductos de admisión de longitud variable pueden cambiar entre dos o más longitudes en diferentes velocidades del motor para optimizar el rendimiento.

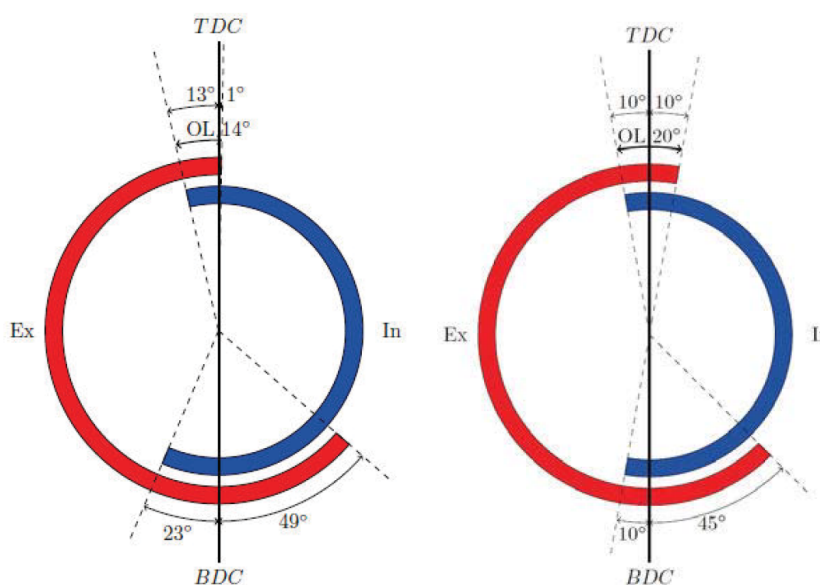
El objetivo de este proyecto es analizar las ondas de presión producidas por el motor durante la apertura de la válvula de admisión y estudiar la longitud idónea del colector de admisión para el motor Ecocar de DTU Roadrunners. El fin consiste en lograr que la llegada de la onda de compresión ocurra en el momento preciso para introducir más aire en el cilindro y conseguir una mayor eficiencia volumétrica. La longitud del conducto de admisión se estudia para diferentes velocidades del motor y dos árboles de levas distintos.

2.- Metodología

En primer lugar, se describe la física de las ondas de presión para comprender el comportamiento de las ondas al propagarse por los conductos. Se analiza la velocidad de propagación de las ondas de presión y su relación de presión, así como las variaciones que se producen cuando la onda de presión alcanza un extremo cerrado o abierto. El extremo abierto es el de mayor interés, por el hecho de que este representa la situación que se encuentra la onda de expansión, producida por la válvula de admisión al comienzo de la carrera de admisión, cuando llega al final del conducto de admisión. La onda de expansión alcanza el extremo abierto del conducto y se refleja como una onda de compresión, cuya relación de presión está por encima de la atmosférica. En segundo lugar, se describe la ecuación que determina la longitud ideal del colector de admisión. La longitud ideal, que se muestra a continuación, depende del régimen del motor, de la duración de la válvula de admisión y de la velocidad acústica.

$$L = a \cdot \frac{1}{2} \cdot \frac{\Delta\theta \cdot 60}{N \cdot 360^\circ}$$

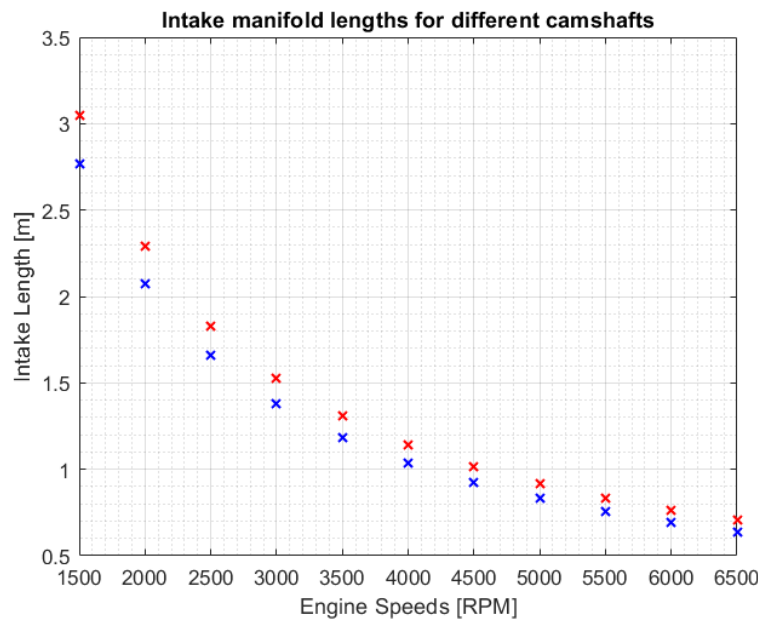
Los datos utilizados para la distribución de las válvulas corresponden a los árboles de levas construidos para el motor Ecocar en DTU. Los árboles de levas tienen diferentes tiempos de apertura de las válvulas de admisión que darán como resultado diferentes longitudes de los conductos de admisión para las mismas velocidades del motor.



3.- Resultados

La longitud ideal del colector de admisión para producir el efecto resonante depende de la duración de la válvula de admisión y de la velocidad del motor. Para duraciones más cortas de la válvula de admisión, la onda de presión tiene menos tiempo para llegar, por lo tanto, el conducto de admisión debe ser más corto, mientras que para duraciones más largas de la válvula de admisión ocurre lo contrario. En cuanto a la velocidad del motor, las revoluciones por minuto más bajas dan como resultado longitudes de los conductos de admisión más largas, mientras que revoluciones por minuto más altas acortan la longitud del conducto de admisión, ya que la onda de presión tiene que llegar más rápido al puerto de admisión.

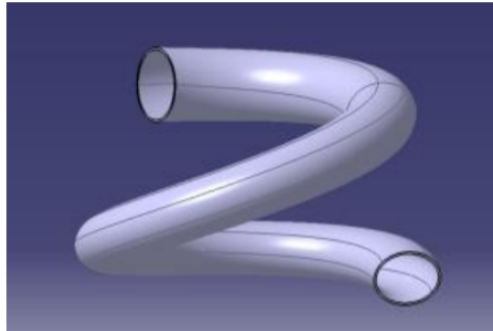
El árbol de levas con mayor duración de la válvula de admisión necesita longitudes de colector más largas para lograr el efecto resonante. Ambos árboles de levas requieren conductos de admisión excesivamente largos a bajas revoluciones del motor, alcanzando longitudes de hasta 3 m. Por el contrario, para velocidades de motor más altas, la longitud del colector de admisión disminuye a valores dentro del rango de 0,5 a 1 m, lo cual es aceptable.



4.- Conclusiones

El motor del Ecocar no puede competir a velocidades superiores a las 3750 revoluciones por minuto, por lo que se esperan colectores de admisión más largos. Como solución a este problema, se propone un colector de admisión helicoidal, en lugar del tubo recto estándar. El conducto de forma helicoidal satisfaría los requisitos de longitud manteniendo un tamaño compacto. Además, la turbulencia producida por la forma helicoidal mejoraría la mezcla de aire y combustible, lo que también puede tener un impacto en el rendimiento. Puede que no valga la pena fabricar el conducto de admisión en hierro fundido, debido a las bajas velocidades del motor a las que

funciona el motor Ecocar y al efecto reducido de las ondas de presión a esas revoluciones. El corredor podría fabricarse en DTU mediante fabricación aditiva utilizando ABS P400, en lugar de hierro fundido, con el fin de reducir el peso y aumentar la relación potencia / peso.



PRESSURE WAVES ANALYSIS FOR INTERNAL COMBUSTION ENGINE OPTIMIZATION

Author: Loureiro Orejas, Álvaro.

Director: Jesper Schramm.

Collaborating Institution: Danmarks Tekniske Universitet.

PROJECT SUMMARY

1.- Introduction

Four-stroke internal combustion engines extract power from the combustion of air and fuel, but only one of the strokes generates power: the expansion stroke. The rest of the strokes prepare the engine for the expansion stroke: the intake stroke fills the cylinder with air and fuel, the compression stroke raises the pressure of the cylinder before the expansion stroke extracts the power and the exhaust stroke drains the results of combustion out of the cylinder, preparing the engine for another cycle.

The power obtained at the crankshaft depends on the amount of fuel burned, which is constant due to the air-fuel ratio. However, if the air introduced in the cylinder at the intake stroke increases, more fuel can be burned, thus, the brake power would increase.

In order to achieve the latter, manufacturers have designed several mechanisms to try to improve their internal combustion engines capabilities. There are different paths leading to an improvement in the air exchange and filling of the cylinder, but two of the most important are the variable valve timing and the variable length intake manifold. The variable valve timing systems outperform standard valve timings due to the capability of changing the duration and timing of the intake and exhaust valves. When running at high engine speeds, the engine requires longer opening times than when the engine is running at lower speeds. Variable valve timing systems can switch at a certain engine speed from one configuration to another, improving the performance of the engine.

Variable length intake manifolds take advantage of the pressure waves produced by the engine to raise the intake port pressure at the intake ramming area, when the intake valve is closing. The particularity of this system is that it varies its length depending on the engine speed to improve the pressure charging. While constant length intake runners may be detrimental at certain engine speeds, the variable length intake runners can switch between two or more lengths for different engine speeds to optimize performance.

The objective of this project is to analyze the pressure waves produced by the engine at the intake valve opening and study the desired intake manifold length for the Ecocar engine of DTU

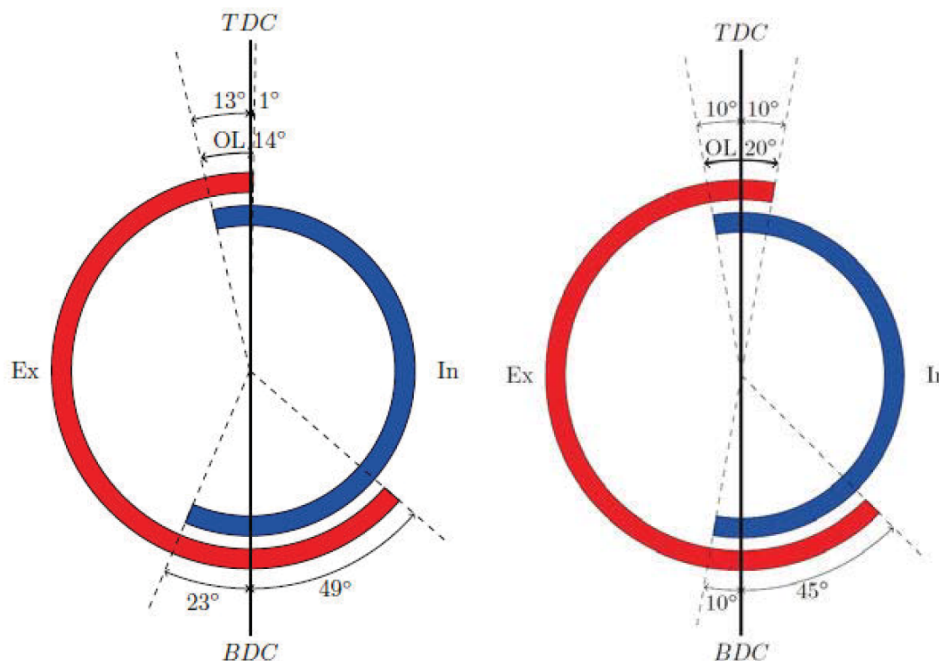
Roadrunners in order to achieve a beneficial arrival of the compression wave for an increased volumetric efficiency. The length of the intake runner is studied for different engine speeds and two valve timings.

2.- Methodology

Firstly, the pressure waves physics is described in order to comprehend the behaviour of the waves when propagating through the ducts. The propagation velocity of the pressure waves and their pressure ratio is analyzed, as well as the variations produced when the pressure wave reaches a closed end or an open end. The open end is of most interest, due to the fact that it represents the situation encountered by the expansion wave produced by the intake valve at the beginning of the intake stroke. The expansion wave reaches the open end of the duct and reflects as a compression wave, whose pressure ratio is above the atmospheric. Secondly, the equation that determines the intake manifold length is described. The latter, shown below, depends on the engine speed, the intake valve duration and the acoustic velocity.

$$L = a \cdot \frac{1}{2} \cdot \frac{\Delta\theta \cdot 60}{N \cdot 360^\circ}$$

The data used for the valve timings corresponds to the camshafts built for the Ecocar engine at DTU. The camshafts have different intake valve durations that will result in different intake runner lengths for the same engine speeds.

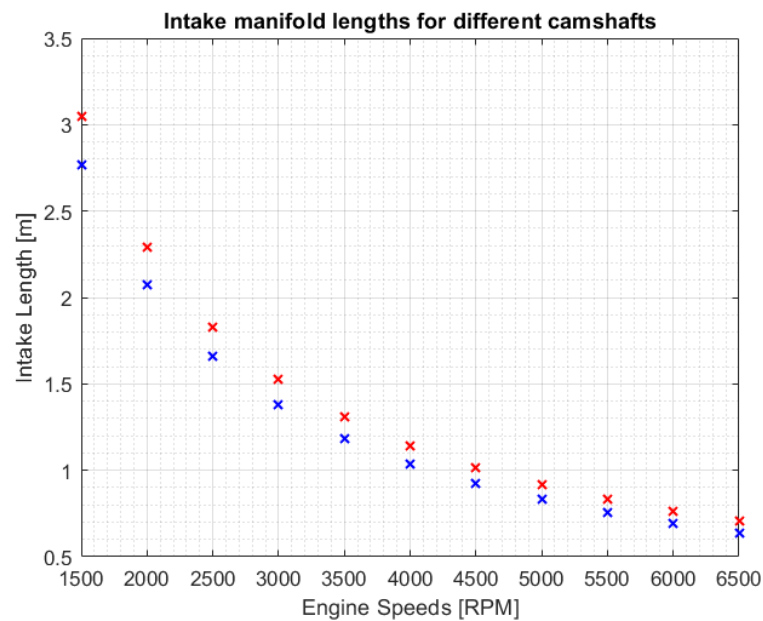


3.- Results

The ideal intake manifold length to produce pressure charging depends on the intake valve duration and the engine speed. For shorter intake valve durations, the pressure wave has less time

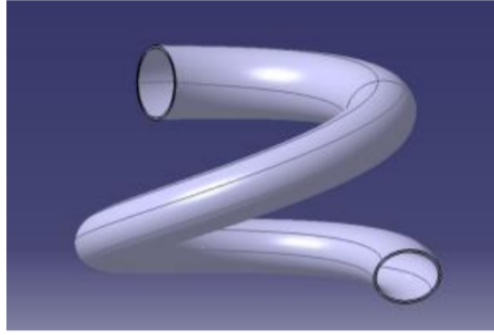
to arrive, therefore the intake runner must be shorter, whereas for longer intake valve durations, the opposite happens. Regarding the engine speed, lower revolutions per minute result in longer intake runner lengths, while higher revolutions per minute shorten the intake manifold length, as the pressure wave has to arrive to the intake port faster.

The camshaft with longer duration of the intake valve need longer manifold lengths to achieve pressure charging at the intake ramming area. Both camshafts require excessively long intake runners at low engine speeds, reaching up to 3 m. On the contrary, for higher engine speeds the intake manifold length decreases to values within the 0.5 to 1 m range, which is acceptable.



4.- Conclusions

The Ecocar engine can not run at engine speeds superior to 3750 revolutions per minute, therefore, longer intake manifolds are expected. To overcome this problem, an helical intake manifold is purposed, instead of the standard straight pipe. The helical shaped runner would satisfy the length requirements while keeping a compact size. In addition, the swirl produced by this shape would improve the mix of air and fuel which may also have an impact on the performance. Manufacturing the intake runner in cast iron may not be worth it, due to the low engine speeds at which the Ecocar engine works and the reduced effect of pressure waves at those revolutions. The runner could be manufactured at DTU by additive manufacturing using ABS P400, instead of cast iron, with the purpose of reducing weight and increasing the power to weight ratio.



Contents

1	Introduction and description of the project	1
1.1	Introduction to ICE parameters	1
1.2	Pressure waves benefits	5
1.3	Valve timing relevance	6
2	State of the art	9
2.1	Variable valve timing	9
2.2	Intake and exhaust optimization	10
3	Description of the developed model	15
3.1	Pressure waves theory	15
3.1.1	Pressure waves superposition	17
3.2	Wave reflections	19
3.2.1	Closed end	19
3.2.2	Open end	20
3.3	Estimated length of the intake manifold for intake ramming	21
3.4	Data	22
4	Results analysis	25
4.1	Base case results	25
4.2	Sensibility analysis	29
5	Conclusions	31
5.1	Methodology conclusions	31
5.2	Results conclusions	31
5.3	Recommendations for future research	33
6	Economic assessment	35
7	Appendix A: Sustainable Development Goals	39

List of Figures

1	The four strokes of an engine [1].	2
2	p - V diagram for an ideal Otto cycle [2]	3
3	The blowdown, pumping, and intake ramming time-areas [4].	5
4	Different intake valve timing configurations and its effect on power and b_{mep}	6
5	Different exhaust valve timing configurations and its effect on power and b_{mep}	7
6	VTEC system by Honda [5].	10
7	Brake power and torque for different intake manifold lengths	11
8	Brake power and brake torque for different intake manifold lengths	11
9	Dual length system designed by Opel	12
10	Variable intake manifold designed by Audi	13
11	Variable intake manifold designed by Volkswagen AG [6].	13
12	Compression wave propagating through a pipe.	17
13	Expansion wave propagating through a pipe.	18
14	Compression wave and expansion wave encounter.	18
15	Illustration of the superposition process.	19
16	Valve timing of the different camshafts.	23
17	Ideal arrival of the pressure wave for D1 camshaft configuration.	26
18	Ideal arrival of the pressure wave for s10 camshaft configuration.	26
19	Intake manifold length for different engine speeds for the D1 camshaft configuration.	27
20	Intake manifold length for different engine speeds for the s10 camshaft configuration.	28
21	Intake manifold length for different engine speeds for the s10 and D1 camshaft configurations.	29
22	Intake manifold length for different engine speeds and valve timing configurations.	30
23	Kistler sensor type 601A [9].	31
24	Helical runner.	32
25	Torque of the s10 (blue and orange) and D1 (grey) camshafts by [8].	34
26	Norway average fleet CO2 emissions for new passenger cars [18].	39

List of Tables

1	Shell EcoMarathon Engine specifications	22
2	Intake lengths from Figure 19.	27
3	Intake lengths from Figure 20.	28
4	Manifold lengths for various engine speeds and pressure waves arrivals	30
5	Cast iron and ABS prices and densities.	35
6	Savings in fuel due to improved efficiencies	36

Abbreviations list

ABDC: After Bottom Dead Center.

ATDC: After Top Dead Center.

BBDC: Before Bottom Dead Center.

BDC: Bottom Dead Center.

BP: Brake Power.

bsfc: Brake specific fuel consumption.

BTDC: Before Top Dead Center.

DTU: Danmarks Tekniske Universitet.

EVC: Exhaust Valve Closing.

EVO: Exhaust Valve Opening.

FA: Fuel to air ratio.

FP: Friction Power.

IP: Indicated Power.

IVC: Intake Valve Closing.

IVO: Intake Valve Opening.

M: Molecular mass.

N: Revolutions per minute.

p: Pressure [Pa].

RPM: Revolutions per minute.

T: Temperature [K].

t: Time [s].

TDC: Top Dead Center.

u: Local velocity [m/s].

X: Pressure amplitude ratio.

a_o: Acoustic velocity at the reference conditions [m/s].

H_u: Lower heating value [kJ/kg].

\dot{m}_f : Mixture flow at the intake valve [kg/s]

p_o : Pressure at the reference conditions [Pa].

R_o : Ideal gas constant [kJ/(K· kmol)]

1 Introduction and description of the project

1.1 Introduction to ICE parameters

Internal combustion engines convert energy from fuel to mechanical work using the products of the combustion directly. Therefore, this type of engines do not require heat exchange to work, as the combustion of the fuel and the oxidizer produce the work without any heat exchange involved. On the contrary, external combustion engines use combustion to heat the working fluid in order to obtain mechanical work.

Internal combustion engines working with a piston can be classified into two stroke or four stroke engines. Four stroke engines need four strokes in order to complete one cycle, as shown in Figure 1. Each stroke has its own characteristics, further explained below.

- **Intake:** The piston moves from the Top Dead Center (TDC) to the Bottom Dead Center (BDC), lowering the pressure. The intake valve is opened in order to introduce a new mixture of air and fuel into the cylinder.
- **Compression:** The piston moves upwards and compresses the gases, increasing their temperature and pressure by reducing their volume. The intake valve is closed, so the gases can not leave the cylinder.
- **Power or expansion:** When the piston reaches TDC, the spark plug starts the ignition of the compressed mixture and provokes the detonation, increasing both the pressure and the temperature. The high pressure gases move the piston downwards and generates motion at the crankshaft.
- **Exhaust:** The piston moves upwards again and the exhaust valve opens in order to exhaust all the residual gases produced in the combustion.

These engines produce power by burning a mixture of air and fuel in a combustion chamber created by the cylinder and the piston. When the mixture explodes, the piston moves down due to the high pressure gases generated in the combustion process.

The pressure-volume diagram is a chart in which the pressure of the cylinder varies with its volume, as piston moves upwards and downwards reducing and increasing the volume of the cylinder. The different strokes of the engine can be easily identified in this diagram, shown in Figure 2. From (1) to (2) the piston compresses the air, ideally causing an adiabatic compression. At TDC, (2) to (3), the spark plug is activated and produces the combustion, raising the pressure at constant volume. The piston moves downwards and producing work, which is given by the

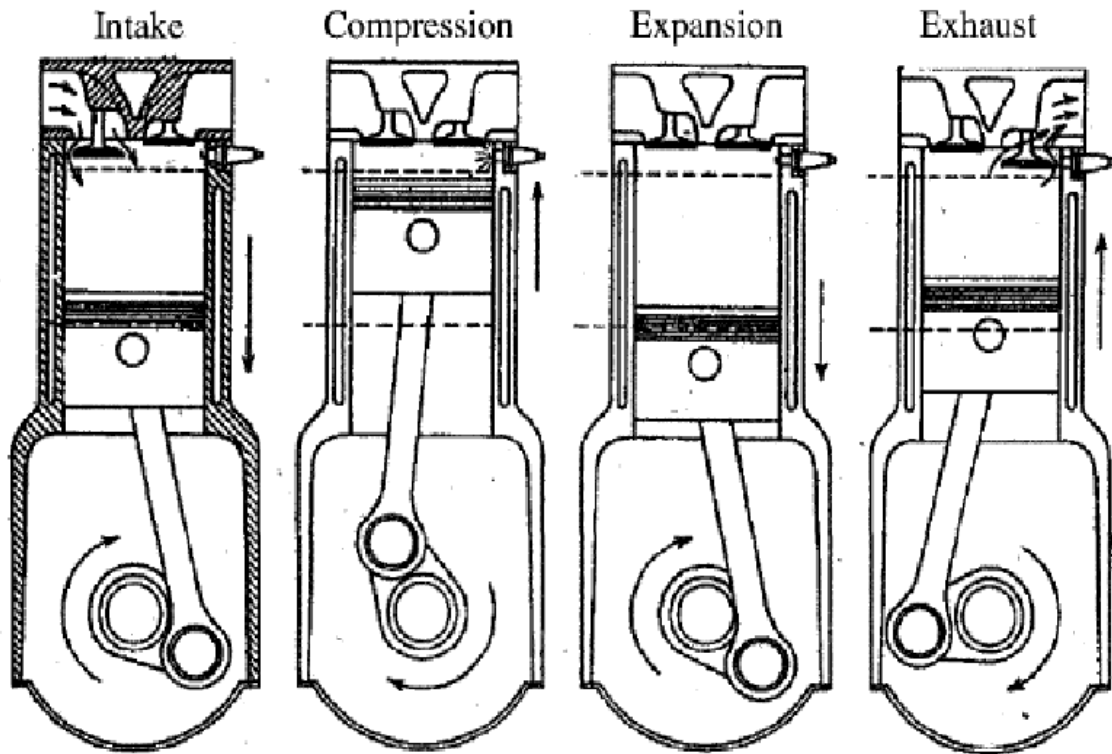


Figure 1. The four strokes of an engine [1].

area enclosed by the cycle; it is represented by (3) to (4). It can be assumed that there is no heat exchange with the environment, due to the rapid expansion, therefore, the ideal process is considered adiabatic. During expansion, the volume increases and the pressure and temperature decrease. The exhaust is represented by (4) to (1).

The fuel burned per cycle determines the power output from the engine at a given speed. For a constant fuel-air ratio, the amount of air introduced in the cylinder will regulate the amount of fuel burned. If the amount of air introduced in the cylinder is increased, higher power output can be obtained from the engine. Thus, air exchange in internal combustion engines is a decisive factor in terms of power optimization, as it plays an important role in combustion, hence, in power output.

The energy obtained from the fuel between compression and expansion is defined as indicated work. This energy will not be translated directly into power to the shaft, as there are pumping losses and friction.

$$W_i = \int_{BDC_{comp}}^{BDC_{exp}} p \cdot dV \quad (1)$$

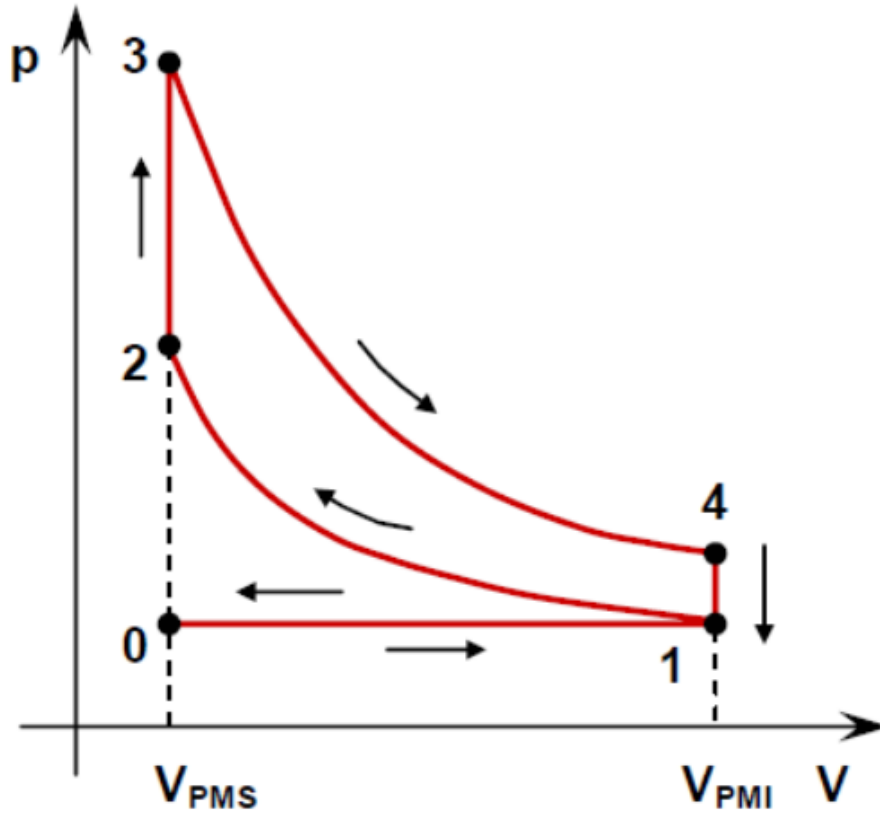


Figure 2. p - V diagram for an ideal Otto cycle [2]

The power produced on top of the piston is called indicated power. Some of the indicated power will be used to start the cycle again by overcoming the pumping losses and friction. The remainder power, called brake power, will be exploited by the output shaft.

$$IP = BP - FP \quad (2)$$

As mentioned before, the engine obtains energy from the fuel. The input energy depends on the fuel flow introduced in the engine and on the lower heating value of the fuel, as shown in Equation (3).

$$Q_{in} = \dot{m}_f \cdot H_u \quad (3)$$

The brake engine thermal efficiency, denoted as η_e , determines the amount of fuel energy transformed to brake power. It is defined as:

$$\eta_e = \frac{BP}{\dot{m}_f \cdot H_u} \quad (4)$$

If fuel efficiency wants to be improved, the most important parameter is the brake specific fuel consumption, defined as the ratio between the fuel flow and the brake power.

$$bsfc = \frac{\dot{m}_f}{BP} \quad (5)$$

According to Spencer C. Sorenson [3], the ideal flow of air at the intake stroke for a four stroke engine is:

$$\dot{m}_{a,in} = \frac{V_d \cdot \rho_{in} \cdot N}{60 \cdot x} \quad (6)$$

The air flow depends on the volume displacement swept by the cylinder, but the process is not perfect. The ratio between the actual air flow and the ideal air flow is defined as volumetric efficiency.

$$\eta_v = \frac{\dot{m}_a}{\dot{m}_{air,ideal}} = \dot{m}_a \cdot \frac{60 \cdot x}{\rho_{in} \cdot V_d \cdot N} \quad (7)$$

By implementing the equations given above, the brake power can be defined in the terms shown in Equation (8).

$$BP = \eta_v \cdot \rho_{in} \cdot \frac{V_d \cdot N}{120} \cdot FA \cdot H_u \cdot \eta_e \quad (8)$$

Given the previous expression, the brake power depends on the volumetric efficiency, the intake density and several fixed values, such as the fuel air ratio, the lower heating value of the fuel H_u and the brake engine thermal efficiency η_e . The objective will be to reduce the brake specific fuel consumption by increasing the brake power. In order to do so, intake air must increase its density so greater mass of air is introduced into the cylinder.

Some engines use turbochargers to achieve the latter; a turbine driven by the exhaust gasses increases the pressure of the intake air, enhancing brake power. Other engines use superchargers, which use the same principle as the turbocharger but, in this case, the device is mechanically driven by the crankshaft of the engine. Even though they do not reach the volumetric efficiencies that the previous devices have, naturally aspirated engines can also take advantage of pressure charging by using the pressure waves generated by the engine.

1.2 Pressure waves benefits

When the engine is running, pressure waves are generated in both the intake and exhaust manifolds due to flow variations. These flow variations are caused by the piston moving upwards and downwards and by the intake and exhaust valves. The pressure waves cause changes in velocity and pressure, depending on the characteristics of the flow in which they propagate. The pressure waves generated at the intake port and its synchronization with the valve openings will boost the pressure and introduce more air in the cylinder, producing an increased air flow and enhancing brake power. This will happen if a pressure wave with a pressure ratio greater than the atmospheric reaches the intake port just after BDC, when the intake valve is moving downwards. It is shown in Figure 3, where the intake ramming area corresponds to the ideal time for the pressure wave arrival, between BDC and the intake valve closing or IVC.

The pressure waves generated at the exhaust port can also be used to improve the air exchange process and the performance of the engine. The latter is called scavenging and it is also shown in Figure 3. The exhaust blow down occurs between the exhaust valve opening or EVO and BDC, where the piston is still moving downwards and concluding the power stroke. If an expansion wave reaches the exhaust port between EVO and BDC, an increased amount of gasses will exit the cylinder, decreasing the pressure of the exhaust pumping stroke and therefore reducing the power needed to clear the cylinder. However, if the expansion wave arrival is not synchronized correctly, it can be disadvantageous, as it could lead to different undesirable situations: firstly, more gasses will be kept in the cylinder, which will increase the pumping work; secondly, if not all the gasses are exhausted, they will mix with the intake air, reducing the amount of air that can be ingested during the intake process and decreasing the performance of the engine.

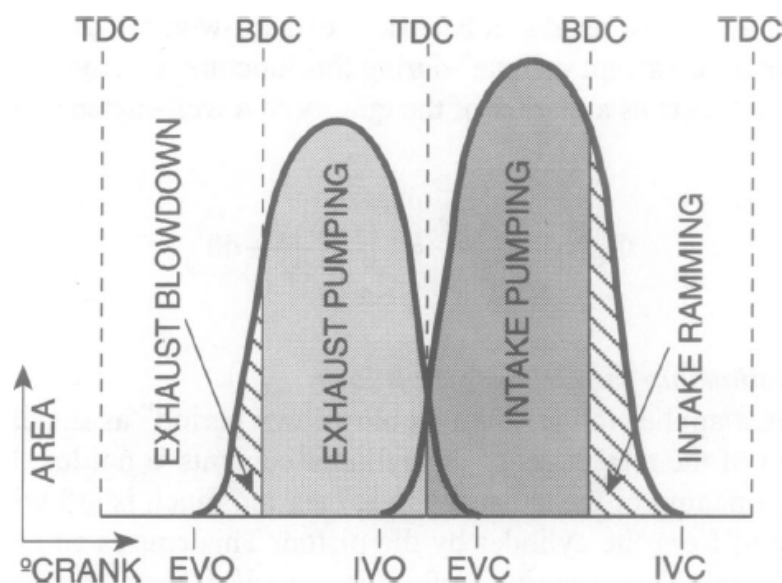


Figure 3. The blowdown, pumping, and intake ramming time-areas [4].

1.3 Valve timing relevance

In an ideal process, the intake valve would open exactly at TDC, when all the exhaust gasses exit the cylinder, and close exactly at BDC, before the piston moves upwards again to start the compression stroke. The exhaust valve would open at BDC just after the power stroke and close at TDC before the start of the intake stroke. In reality, this cannot happen, due to the fact that valves are driven by cams that can not withstand infinite forces. For this reason, both valves open and close in a smooth way, as it can be seen in Figure 3. In addition, each valve must be opened as much as possible when the piston speed is maximum in order to maximize the flow, therefore, it is beneficial to open the valves slightly before and close them somewhat after, as it is shown in Figures 4 and 5. The graphs show the brake power and *bmep* for different valve timing configurations and engine speeds for a 324cc engine with one cylinder, retrieved from [3]. The early intake opening and the late intake closing increase the brake power at higher speeds, as a high amount of air is required, while at low speeds the differences are not evident. For the exhaust, an early opening of the valve improves the brake power just as it happened with the intake valve, while for the exhaust closing the improvements are minimum.

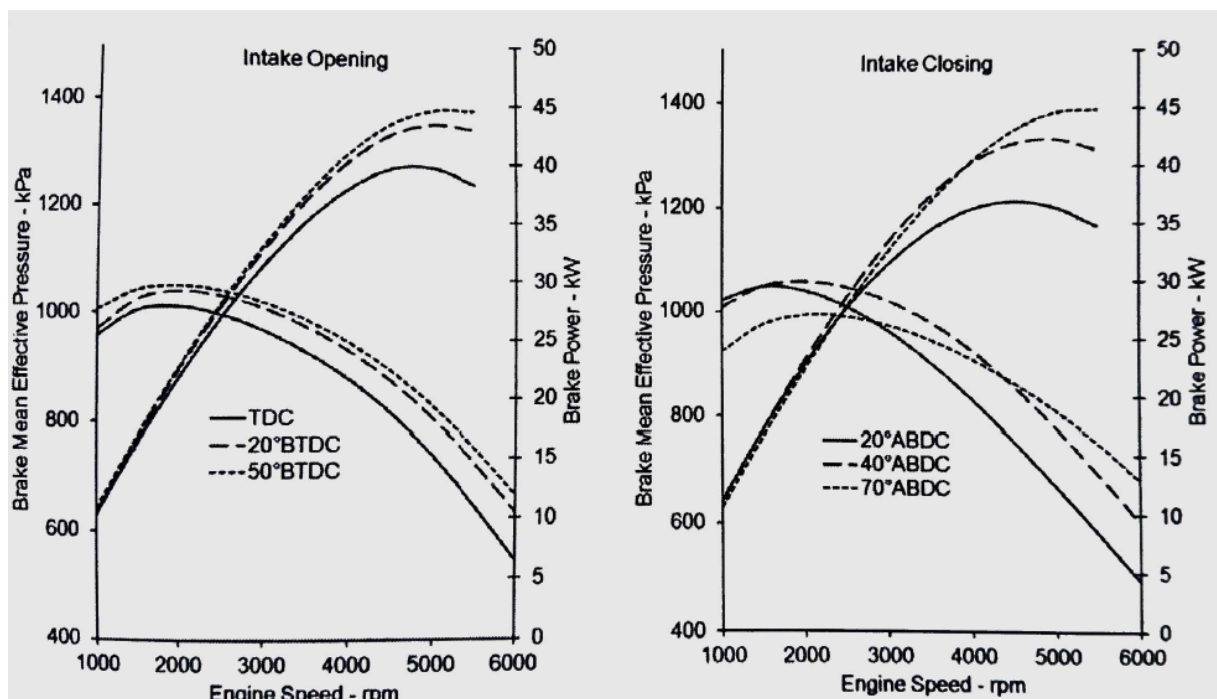


Figure 4. Different intake valve timing configurations and its effect on power and *bmep*.

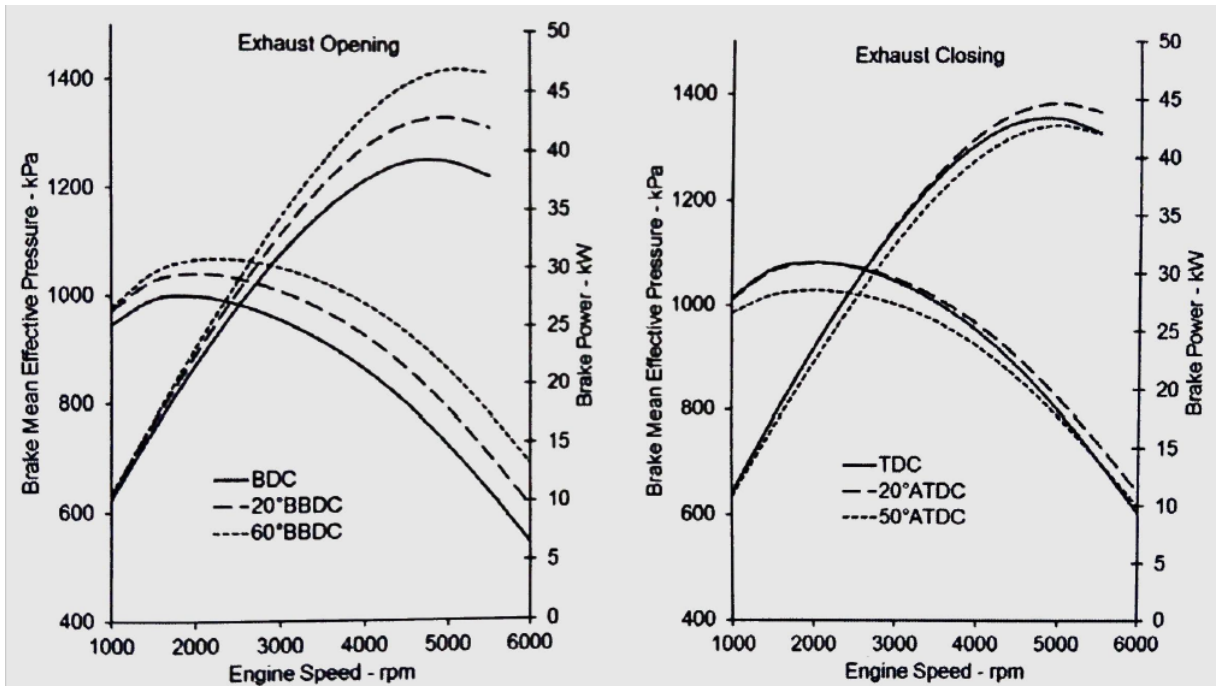


Figure 5. Different exhaust valve timing configurations and its effect on power and *bmep*.

2 State of the art

In order to achieve better volumetric efficiencies, different mechanisms have been developed by the manufacturers. Those mechanisms are usually related to the valves timing and the intake and exhaust ducts; some of them are further explained throughout this section.

2.1 Variable valve timing

At the beginning, internal combustion engines were designed with a constant valve timing. The intake and exhaust valves opened and closed at particular crank angle degrees. This would cause the engine to perform better at a precise range of RPM, while it would underperform out of the range, as explained in the introduction. Thus, variable valve timing was developed in order to improve the engines capabilities throughout the entire range of revolutions and reduce the fuel consumption, as the European emission standards are increasingly strict.

The implementation of variable valve timing systems has not been simple due to its high cost and low reliability, until recent developments. Several manufacturers have developed variable valve timing systems, each with its own particularities and performance. One of the most successful systems is the VTEC (Variable Valve Timing and Lift Electronic Control), developed by Honda Motor Corporation. The system achieves variable valve timing by operating the two intake valves with three cams instead of the usual two, as shown in Figure 6. Cams 1 and 3 have the exact same profile and are designed to optimize fuel consumption and stability, while cam 2 has a different profile, designed to maximize power output at higher engine speeds.

When the engine is running at low RPM, cams 1 and 3 activate their rocker arms which open and close the intake valves, while the rocker arm of cam 3 simply moves up and down, without causing any effect on the intake valves as it is not connected to the two others. When some conditions are met, the ECU switches from cams 1 and 3 to cam 2, which causes an increased lift and extends the duration. In order to do so, the ECU takes into account several inputs, such as the temperature, speed and oil pressure of the engine or the throttle position. If the conditions are met, oil pressure from a spool valve actuated by a solenoid operates a locking pin that connects the rocker arm of cam 2 to the rocker arms of cams 1 and 3. Once they are connected, the intake valve will open and close following the rocker arm actuated by cam 2. The switch-over point is variable, due to the fact that in some situations the engine could be working around the switch-over point and it would be undesirable to be constantly switching between cams. Thus, the high valve lift mode is activated at higher engine speeds than when it is deactivated so the engine works again with low valve lift and duration.

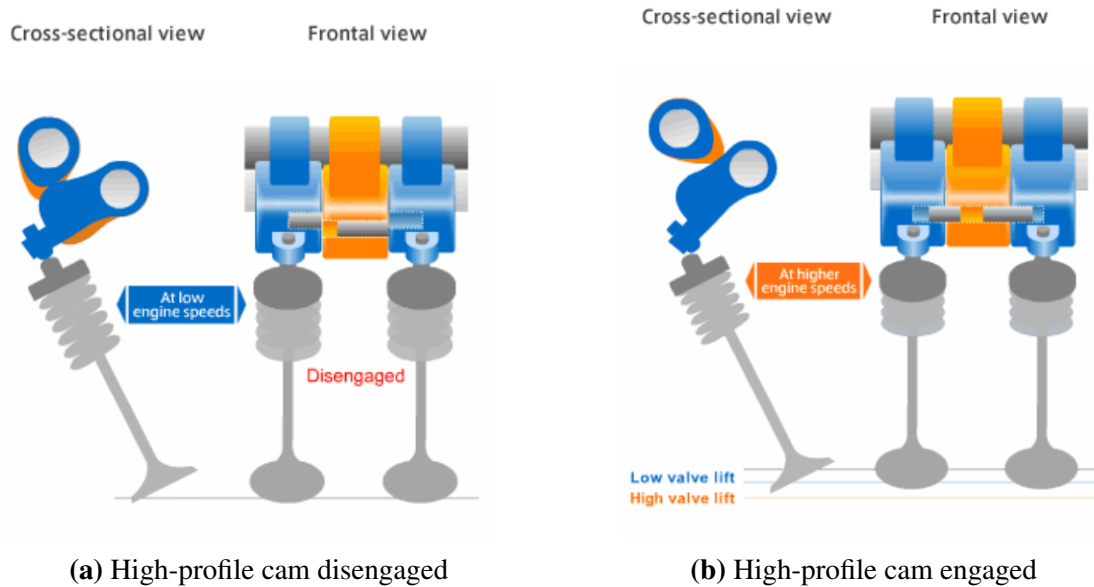


Figure 6. VTEC system by Honda [5].

While the previous system can modify the duration and lift of the intake valve, the phasing remains unaltered. Some manufacturers, such as Toyota with the VVT-i, developed a mechanism to alter the cam phasing and thus, improve the engine performance. This is achieved by allowing the camshaft to rotate with respect to the camshaft drive. The camshaft is driven by a toothed belt or a chain, but a pulley is placed instead of a standard gear. The internal mechanism of the pulley allows different cam phasing and therefore improves the engine capabilities, if the phasing is correctly adjusted to the engine load requirements.

2.2 Intake and exhaust optimization

The optimization of pressure waves caused by the intake and exhaust has an impact on the air exchange process, hence, manufacturers have developed different systems to maximize its advantages. The main idea is to take advantage of the arrival of the compression wave at the intake port, but a fixed manifold length would result in a narrow range of engine speeds in which this effect is noted, as shown in Figure 7, where the torque and brake power of an engine with different intake manifold lengths is shown with respect to the engine speed.

Note that the manifold with the best performance is the 700mm duct up to 4500 rpm; for higher speeds, the 500mm duct performs better. The ideal situation would be to increase the length of the manifold for lower speeds and decrease it when the engine is running at higher speeds. If the latter can be achieved, the torque and brake power graph of the engine would be as shown in Figure 8.

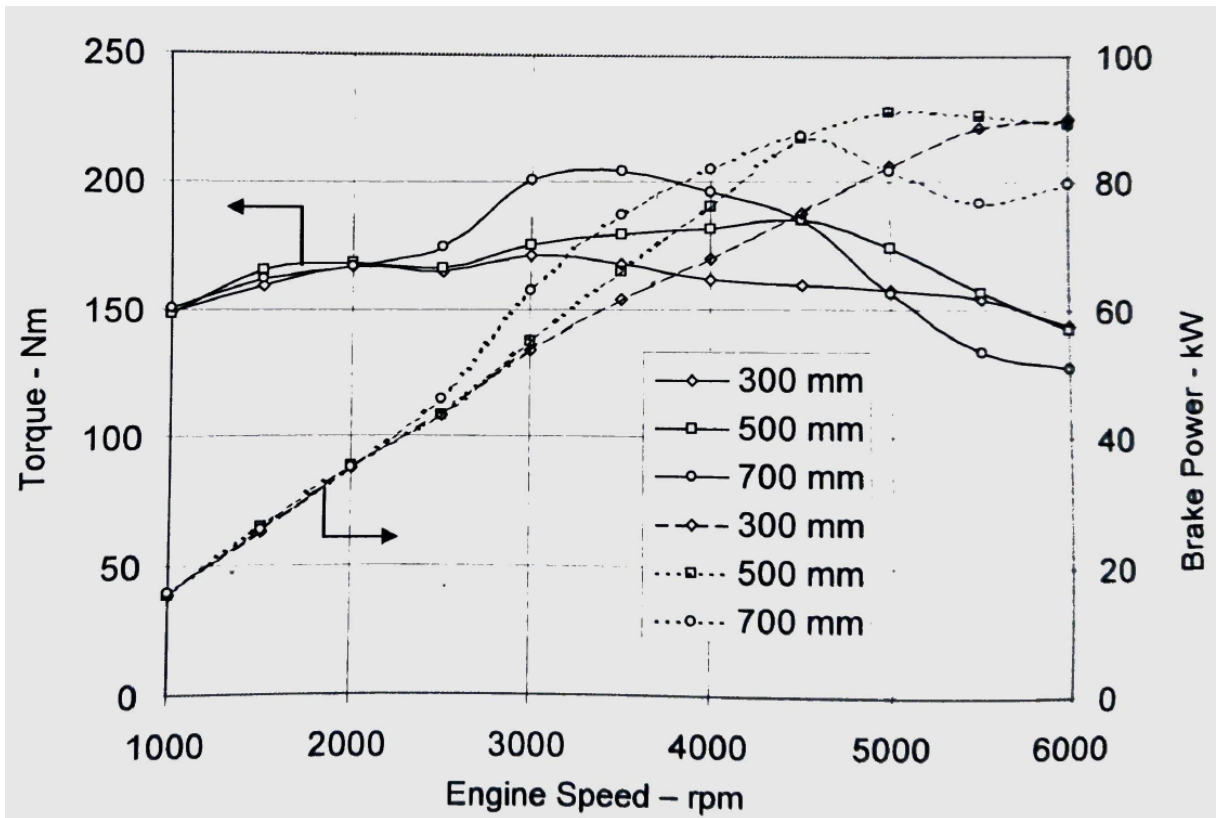


Figure 7. Brake power and torque for different intake manifold lengths

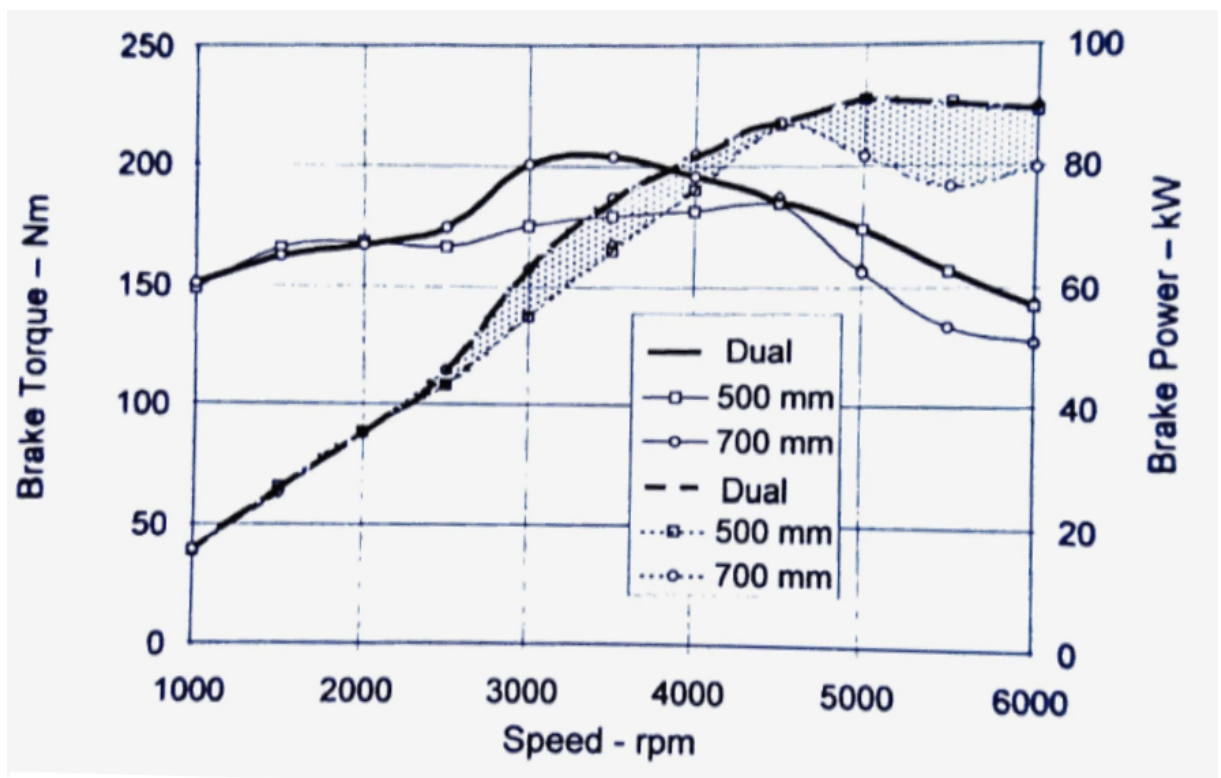


Figure 8. Brake power and brake torque for different intake manifold lengths

Regarding the torque, the result of changing the duct length is a flattened curve and more torque available in a broader range of RPM. With respect to the brake power, it has the same effect, as there is more power available in mid and high RPM.

To achieve the latter, some mechanisms have been developed by the manufacturers. One of the systems, designed by Opel and introduced in one of their 6 cylinder in-line SI engine is shown in Figure 9. The system consists of 6 runners connecting the intake valves to a plenum and the plenum is connected to the throttle plate area, which acts as a second plenum, by 2 runners. In the middle of the plenum there is a valve that when closed, halves the volume of the plenum. When the engine is running at low speeds, the valve closes so the volume of the plenum is reduced and the resonant length becomes longer. When the engine is running at high speeds, it is convenient to shorten the resonant length, so the valve opens in order to increase the plenum volume and decrease the resonant length.

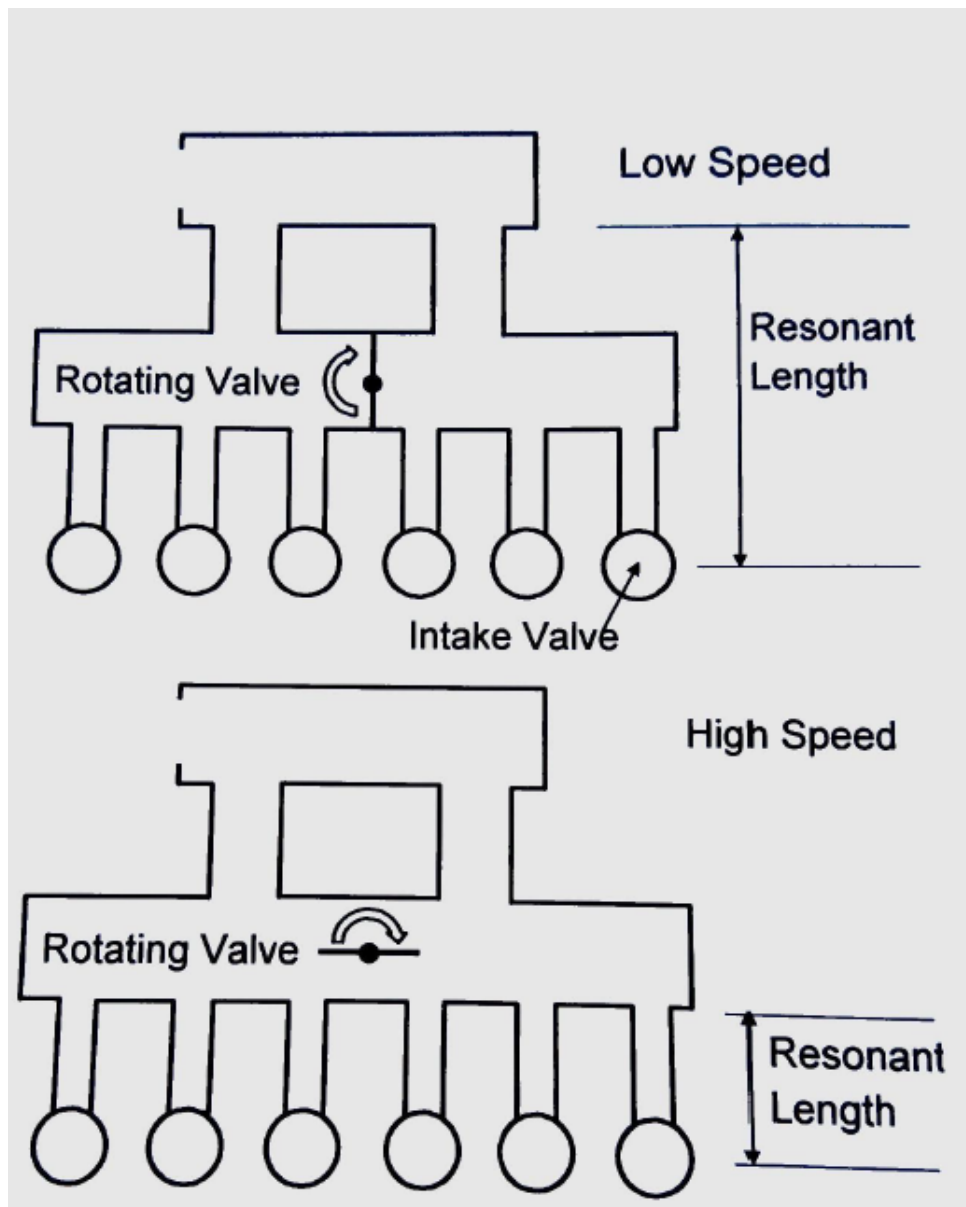


Figure 9. Dual length system designed by Opel

Another system designed for this purpose was designed by Audi. It was designed for a V6 engine, therefore, there was not enough space to design a long configuration as the previous system by Opel. The intake manifold is rounded, as shown in Figure 10, so the runners can lie between the banks of the V6. It has two ducts inside and one valve in each duct, so the air flow can be forced to travel through the desired duct. If the engine is running at low speeds, the short path valve will close in order to force the air flow through the long path. When the engine accelerates to a certain RPM, the air flow is forced to travel through the short path so the resonance enhances the power of the engine. This configuration has been used in other engines of the group, such as the 2.0 FSI from Volkswagen, shown in Figure 11.

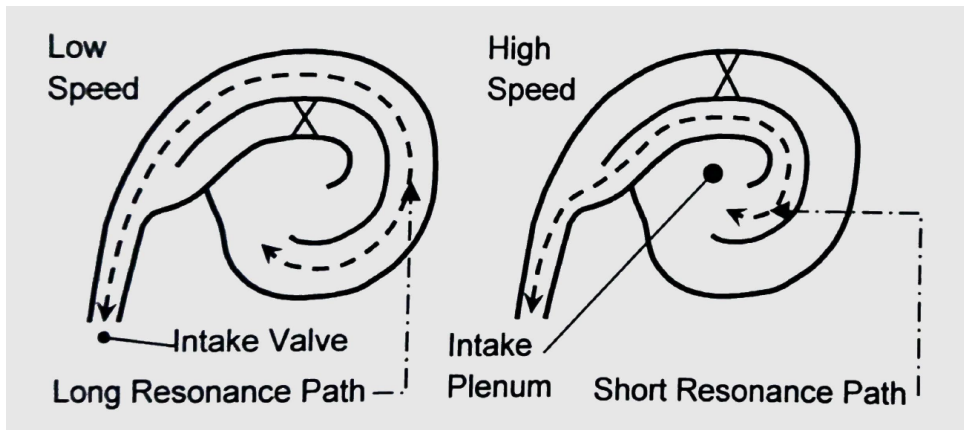
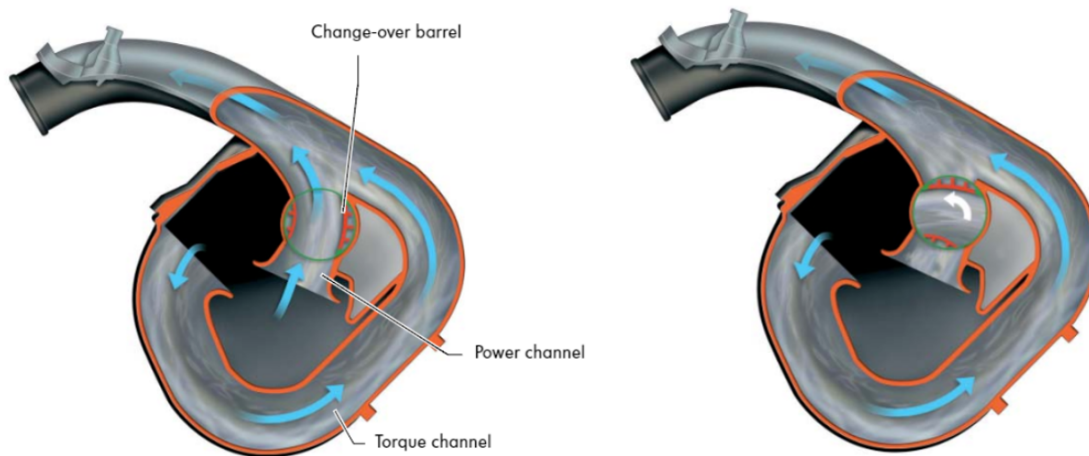


Figure 10. Variable intake manifold designed by Audi



(a) Both ducts opened

(b) Low RPM mode, enhancing torque.

Figure 11. Variable intake manifold designed by Volkswagen AG [6].

3 Description of the developed model

The objective, as said before, is to increase the density of the air at the intake stroke to increase volumetric efficiency. This is achieved by exploiting the benefits of the pressure waves, generated by the engine. A brief description of its physics and behaviour when travelling through pipes will help to understand further calculations. After that, the length of the intake manifold to produce the pressure charging will be studied for different valve timings and engine speeds.

3.1 Pressure waves theory

The speed of a disturbance moving through a gas relative to the local gas velocity will be the speed of sound, therefore, for stationary flow, the disturbance will move at the speed of sound alone. The speed of sound for an ideal gas depends on the specific heat ratio (γ), the molecular weight and the temperature of the gas:

$$a = \sqrt{\frac{\gamma \cdot R_o \cdot T}{M}} \quad (9)$$

The speed of sound can also be defined as an expression depending on density or pressure change, if all the processes taken into account are assumed isentropic:

$$\frac{a}{a_o} = \left(\frac{\rho}{\rho_o}\right)^{\frac{\gamma-1}{2}} = \left(\frac{p}{p_o}\right)^{\frac{\gamma-1}{2\gamma}} \quad (10)$$

A small disturbance in an acoustic wave propagates in both directions, causing density change. If it is assumed that both pressure and density changes are isentropic, the local gas velocity can be obtained by integrating Equation (11) over a change in density, resulting in Equation (12).

$$du = \frac{d\rho}{\rho} \quad (11)$$

$$u = \frac{2a_o}{\gamma-1} \left[\left(\frac{\rho}{\rho_o}\right)^{\frac{\gamma-1}{2}} - 1 \right] = \frac{2a_o}{\gamma-1} \left[\left(\frac{p}{p_o}\right)^{\frac{\gamma-1}{2\gamma}} - 1 \right] = \frac{2}{\gamma-1} \cdot (a - a_o) \quad (12)$$

If the acoustic velocity is moved to the left hand side alone, it can be stated that it changes within the wave, as shown in Equation (13)

$$a = a_o + \frac{\gamma - 1}{2} \cdot u \quad (13)$$

The sum of the local velocity u and the local acoustic velocity a will result in the propagation speed of the wave u_p .

$$u_p = a + u = a_o + \frac{\gamma + 1}{2} \cdot u = a_o \left(1 + \frac{\gamma + 1}{\gamma - 1} \left[\left(\frac{\rho}{\rho_o} \right)^{\frac{\gamma - 1}{2}} - 1 \right] \right) \quad (14)$$

It is important to note that pressure waves propagate relative to the local gas velocity, therefore the absolute velocity will vary along the engine cycle, as the local gas velocity also varies along the engine cycle. The pressure amplitude ratio, denoted as X , is very useful to describe pressure waves and compare between them. It is determined by the local pressure and the atmospheric pressure.

$$X = \left(\frac{p}{p_o} \right)^{\frac{\gamma - 1}{2\gamma}} = \frac{a}{a_o} = \left(\frac{\rho}{\rho_o} \right)^{\frac{\gamma - 1}{2}} \quad (15)$$

If a pressure wave has a pressure ratio greater than one, it is denoted as a compression wave, whereas if the pressure ratio is less than one, it is named a expansion wave. In order to obtain the velocities that define the pressure wave, a pressure ratio must be chosen first. Then, the speed of sound a is calculated from Equation (10) and the local velocity u from Equation (12). After that, the propagation velocity is calculated from Equation (14). When a compression wave propagates through a pipe with quiescent gases, it raises the pressure above atmospheric and moves the gasses through the pipe. The example shown in Figure 12 consists of a compression wave with a local gas velocity u , a wave propagation velocity of u_p and pressure ratio $p = 1.2p_o$. The reference temperature and pressure will be 20°C and 1 atm respectively, therefore the acoustic velocity at the reference conditions is $a_o = 343.23 \text{ m/s}$, following Equation 9.

The local velocity of the gas caused by the increased pressure when the compression wave propagates is positive, therefore the wave provokes a flow of gases in the same direction as the wave propagation. On the contrary, when an expansion wave is propagating through a pipe, the pressure drops and a flow of gases moving in the opposite direction is created, as the local velocity of the gases is negative. A simplified pressure wave of pressure ratio $p = 0.8p_o$ is shown in Figure 13. The procedure to calculate the local gas velocity and the propagation velocity is the same as in the previous calculation regarding the compression wave.

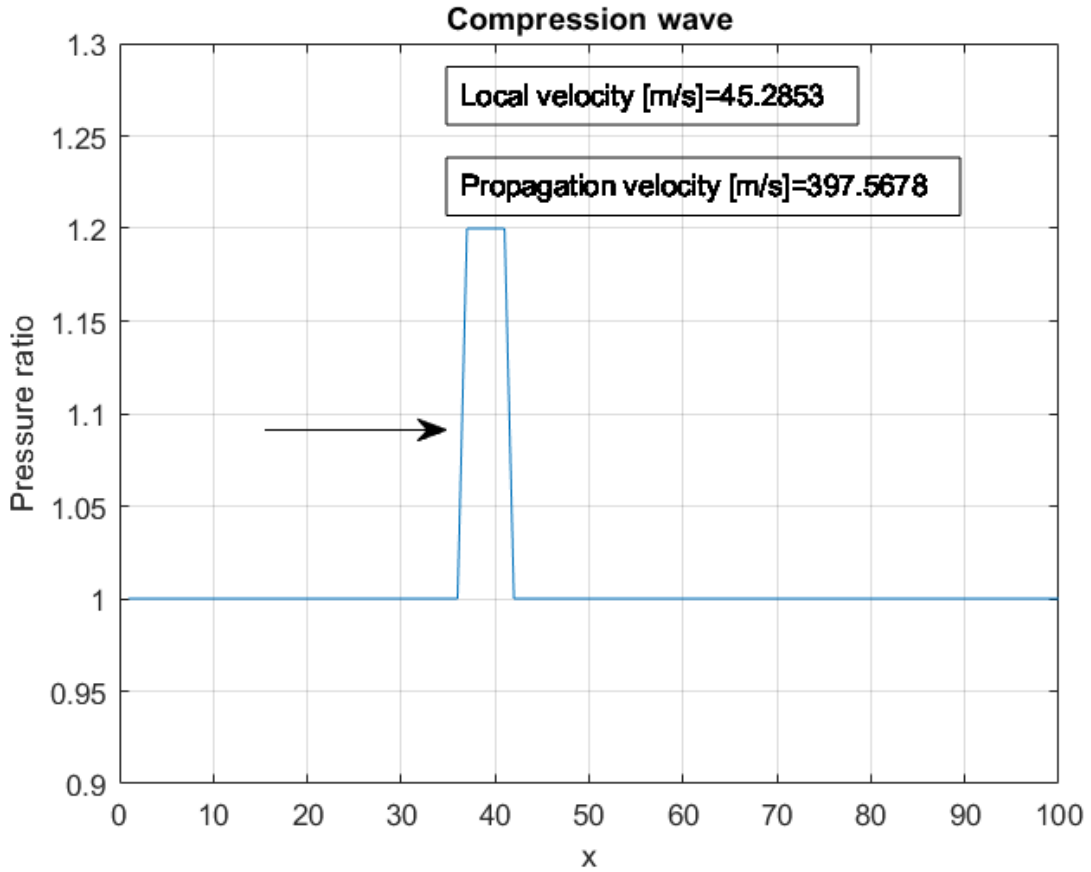


Figure 12. Compression wave propagating through a pipe.

3.1.1 Pressure waves superposition

When two waves meet, the measured pressure ratio and the local velocity at the exact moment in which they meet will change. Therefore, it is interesting to predict the behaviour of the superposition of waves in order to avoid getting confused by the measurement readings. It is possible to calculate the pressure amplitude ratio X_s and the local velocity u_s at the meeting using Equations (16) and Equation (17) respectively.

$$X_s = X_1 + X_2 - 1 \quad (16)$$

$$u_s = \frac{2a_o}{\gamma - 1} (X_1 - 1) - \frac{2a_o}{\gamma - 1} (X_2 - 1) \quad (17)$$

For instance, if a compression wave with a pressure ratio $p = 1.2p_o$ ($X_1 = 1.026$) and an expansion wave with a pressure ratio $p = 0.8p_o$ ($X_2 = 0.9686$) meet in the pipe, the pressure amplitude ratio will be $X_s = 0.995$, thus, the pressure ratio will be $p = 0.9655p_o$. This is illustrated in Figures 14 and 15. The measured pressure ratio at the moment of superposition could lead to a mistake, as in reality there is a compression and an expansion wave with

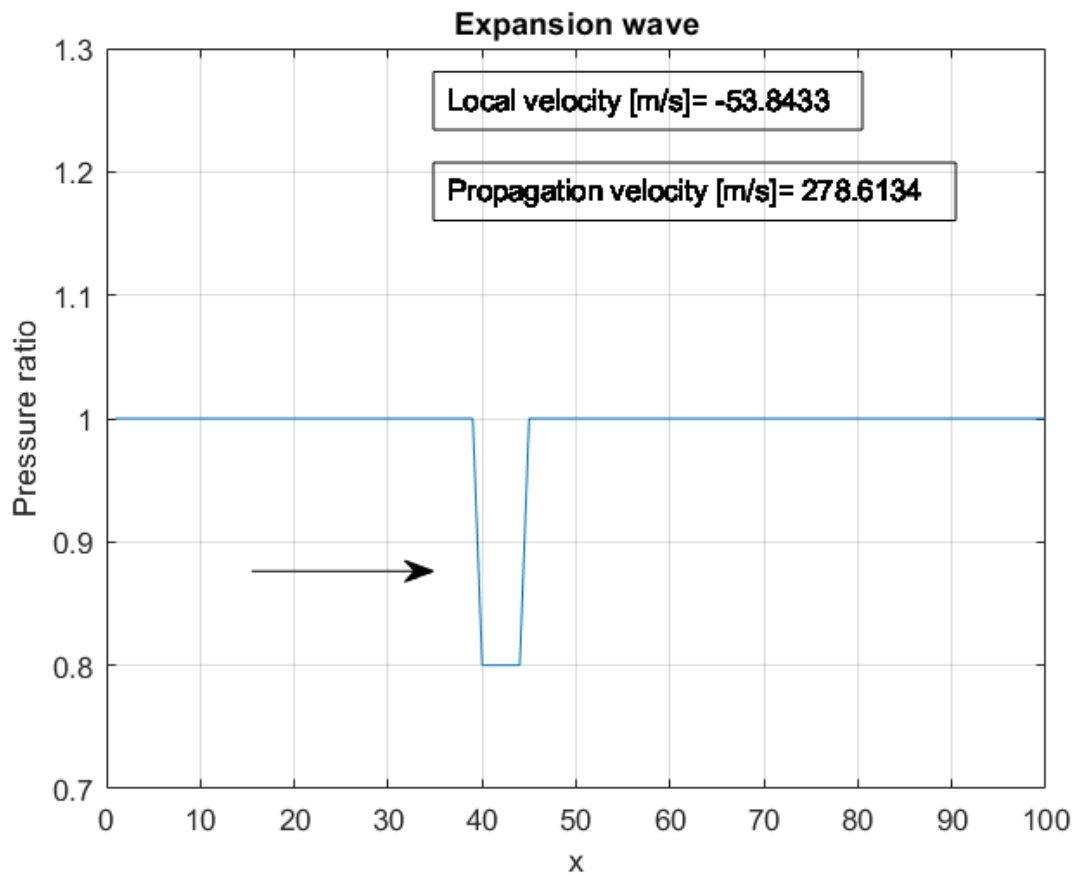


Figure 13. Expansion wave propagating through a pipe.

considerable pressure ratios propagating through the pipe in opposite directions, instead of just the measured expansion wave with a pressure ratio of $p = 0.9655p_o$, which is similar to the atmospheric pressure p_o .

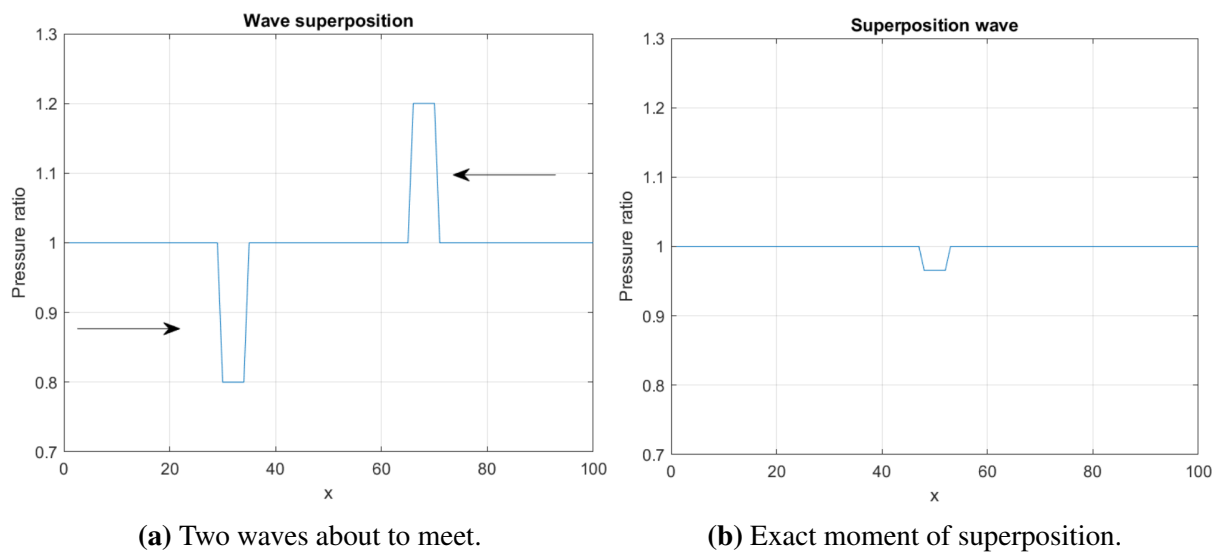


Figure 14. Compression wave and expansion wave encounter.

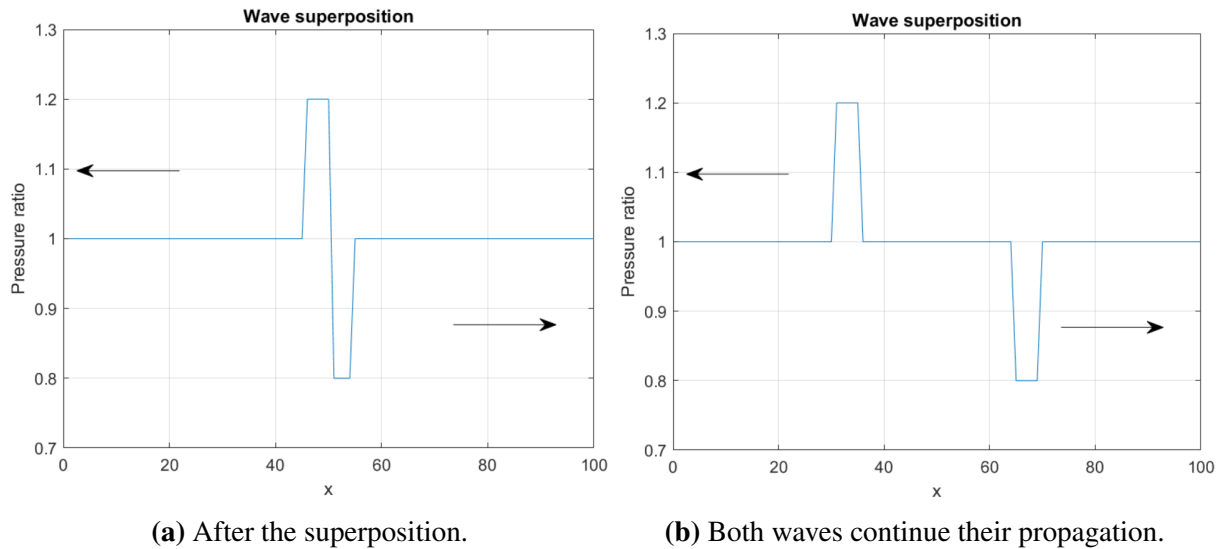


Figure 15. Illustration of the superposition process.

3.2 Wave reflections

When pressure waves encounter variations in the pipe, such as different diameter, a closed pipe or an opening, a reflection occurs. The reflected wave will have different properties than the original wave, depending on the variation encountered. The boundary conditions needed to solve the equations will change depending on the characteristics of the pipe.

3.2.1 Closed end

The speed of the gases at the closed end must be equal to zero. Therefore, when a pressure wave reaches the closed end, another pressure wave with the same velocity modulus but opposite direction takes place. This reflected wave fulfills the condition of zero velocity at the closed end. For instance, a compression wave that is propagating through a closed pipe reaches the end. In this moment, the velocity of propagation and local gas velocity u_s must be zero, therefore, the pressure amplitude ratio X_2 of the reflected wave at the time of superposition can be obtained from Equation (17).

From Equation (16), the pressure amplitude ratio X_s during the time of intersection can be obtained, as well as the pressure ratio p_s , obtained from Equation(15). After the superposition, the reflected wave has the same characteristics as the original wave, but it propagates towards the opposite direction.

3.2.2 Open end

The open end of a pipe can be studied as a reservoir in which pressure stays constant and the velocity of the air is equal to zero, therefore, there will not be propagation of any pressure wave. The pressure of the open end will be considered the atmospheric pressure. When a pressure wave reaches the open end of a pipe, the results will depend on the pressure ratio of the wave; the characteristics of the reflected wave as well as the flow of gas will be different if it is a compression wave or an expansion wave.

If the pressure wave is a compression wave and it is approaching the open end of the pipe, the flow of gas will be positive relative to the direction of propagation of the compression wave. When the compression wave finally reaches the open end, the pressure ratio p_s and pressure amplitude ratio must be equal to one:

$$p_s = 1$$

$$X_s = \left(\frac{p_s}{p_o} \right)^{\frac{\gamma-1}{2\gamma}} = 1$$

The pressure amplitude ratio X_2 of the reflected wave can now be obtained from Equation (16). After obtaining the pressure amplitude ratio, the remaining characteristics of the reflected wave can be easily obtained solving the equations described previously. For example, if a compression wave with a pressure ratio $p = 1.2p_o$ reaches the open end of the pipe, the resulting reflected wave will have the following characteristics:

$$X_2 = 0.9736 \quad p_2 = 0.8292 \quad u = -45.29 \text{ m/s} \quad u_p = 288 \text{ m/s}$$

For the previous case and the following, negative velocities are considered towards the open end. When the wave that approaches the open end of a pipe is a compression wave, the reflected wave will be an expansion wave, as the pressure ratio is lower than 1. The local gas velocity is negative, meaning that the flow of gases will be opposite to the propagation direction of the expansion wave. This will mean that when a compression wave reaches the open end and reflects, the flow of gases will move in the same direction as before, outwards. The reflected wave will be an expansion wave moving in the opposite direction of the original compression wave, inwards.

When the approaching wave is an expansion wave, the flow of gases will go inwards. At the time when it reaches the open end, the expansion wave will reflect and turn into a compression wave. The flow of gases will remain the same, as a compression wave propagating inwards will

provoke a flow of gases in the same direction. For an expansion wave with a pressure ratio of $p = 0.8p_o$ approaching the open end, the reflected compression wave will have the following characteristics:

$$X_2 = 1.031 \quad p_2 = 1.241 \quad u = 53.843 \text{ m/s} \quad u_p = 407.837 \text{ m/s}$$

3.3 Estimated length of the intake manifold for intake ramming

The previous equations are useful to calculate an approximated duration of the propagation of the pressure wave. When the engine starts the intake stroke, the intake valve is opened and the piston is moving downwards, producing the expansion wave. The expansion wave will travel through the manifold towards the open end of the pipe, moving gasses inwards, as previously seen. Once it reaches the open end, the expansion wave will reflect as a compression wave. Intake ramming will be produced if the compression wave arrives at the intake ramming phase, when the piston is starting to move upwards and the intake valve is closing. For the calculations, the expansion wave will be produced exactly at TDC.

There are several parameters that anticipate or delay the pressure wave arrival. The pressure wave propagates through the pipe of length L . It has to cover twice the distance of the pipe, as it is generated in the intake port and it has to arrive to the same point. Thus, the distance to cover will be $2L$. If it is the first cycle, the air is quiescent, therefore, the propagating velocity will be the speed of sound.

As previously mentioned, the propagating velocity of pressure waves is the speed of sound plus the local velocity of the gas. Nevertheless, the propagation velocity of a pressure wave and the reflected wave in a constant air flow will be, on average, the speed of sound. The variations in local velocity of the gasses can be neglected when compared to the acoustic velocity, therefore, it is admissible to approximate the propagation velocity of the wave to the acoustic velocity.

The pressure wave has to travel a distance equal to twice the length of the manifold and arrive to the intake port before the intake valve closes. Thus, the duration of the intake valve timing is an important parameter to consider, as longer durations will increase the length of the manifold. The engine speed is also important, as lower speeds provide more time to the pressure wave, thus, longer intake manifolds. On the contrary, higher engine speeds forces the compression wave to arrive earlier if intake ramming is desired, so the intake manifold should be shorter.

The length of the intake manifold for the intake ramming effect can be determined using Equation 18 [7], where L is the length of the manifold, a is the acoustic velocity at the reference conditions and Δt is the duration of the propagation of the pressure wave.

$$2 \cdot L = a \cdot \Delta t \quad (18)$$

The duration of the propagation must be less than the elapsed time between the intake valve opening and the intake valve closing; if otherwise, the compression wave will arrive when the intake port is closed. Thus, the duration of propagation depends on the valve timing and the engine speed as shown in Equation 19, where Δt is the duration of propagation of the pressure wave, N is the engine speed in RPM and $\Delta\theta$ is the angle between the intake valve opening and the arrival of the pressure wave, measured in crank angle degrees.

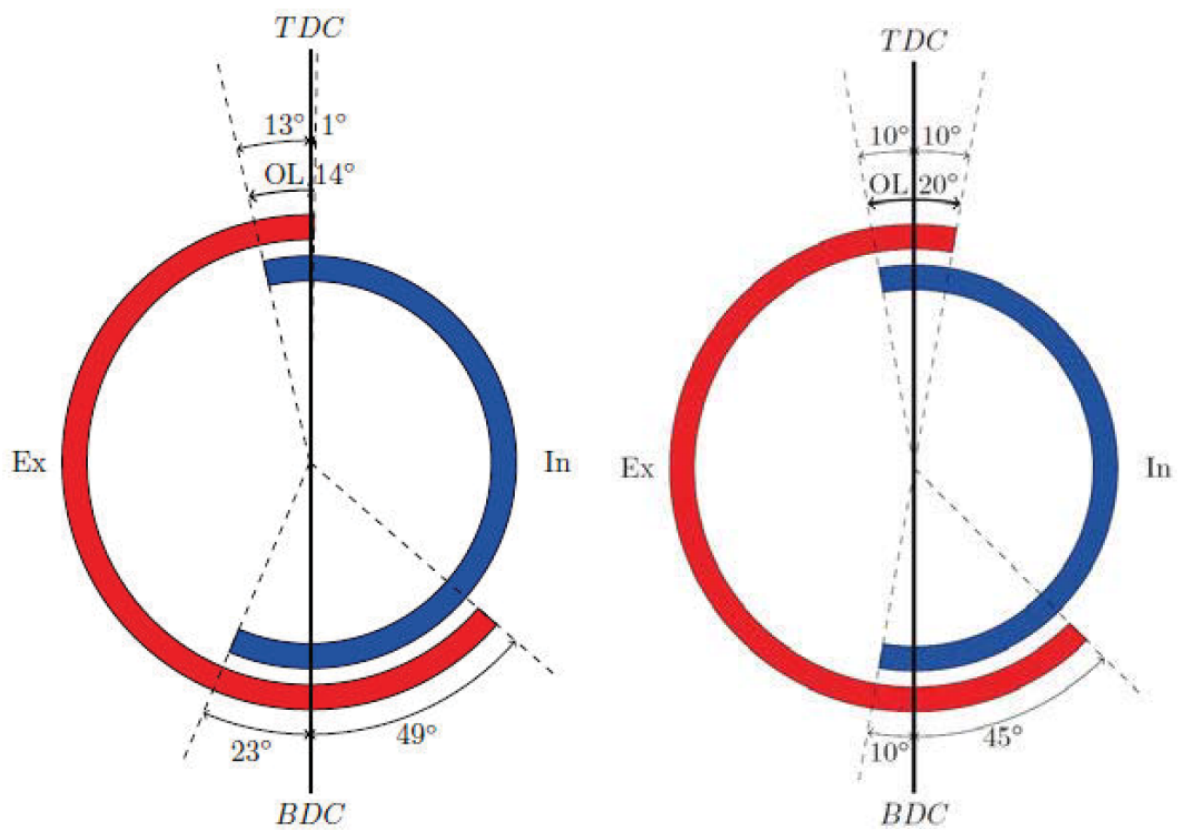
$$\Delta t = \frac{\Delta\theta}{N \cdot 360^\circ \cdot \frac{1}{60}} \quad (19)$$

3.4 Data

The intake manifold length of the DTU Roadrunners engine Legace will be studied. The specifications of the engine are shown in Table 1. The valve timing was studied by Mathias Thage and Gurpreet Singh in [8], where a new designed camshaft was tested together with two older designs. The most efficient camshaft was one of the older designs named D1, whose valve timings are shown in Figure 16a and correspond to the engine specifications. The newer design was named s10 and its valve timings are shown in Figure 16b. For the calculations done in Chapter 4, both valve timings will be used.

Specifications			
Bore	Stroke	Displacement	Compression ratio
35 mm	43.5 mm	42 cm ³	14
IVO	IVC	EVO	EVC
13° BTDC	23° ABDC	49° BBDC	1° ATDC

Table 1. Shell EcoMarathon Engine specifications



(a) Valve timing of the camshaft type D1.

(b) Valve timing of the camshaft type s10.

Figure 16. Valve timing of the different camshafts.

4 Results analysis

4.1 Base case results

If the D1 camshaft is used, the expansion wave produced when the intake valve is opened has to reach the end of the pipe, so it reflects and becomes a compression wave, and arrive before the intake valve closes at 23° after TDC. However, the ideal arrival is not the intake valve closing event, as the peak or pressure would arrive when the intake valve is closed.

The peak pressure has to arrive when the intake valve is descending but still with enough lift to allow the extra air into the cylinder, as shown in Figure 17. The black vertical lines determine the estimated boundaries in which the arrival is desired, set at 140° and 190° . The pressure at the intake port before the intake valve opens is considered atmospheric, even though this only happens in the first cycle. The following cycles have oscillations, depending on engine speed.

The intake valve opens and the gas flow starts to fill the cylinder. The expansion wave produced due to the low pressure at the cylinder after the exhaust stroke reaches the end of the pipe and reflects as a compression wave, reaching the intake port and introducing more air in the cylinder, raising the volumetric efficiency. A similar graph is shown in Figure 18 for the s10 camshaft configuration, although the estimated arrival boundaries have been changed due to the shorter duration of the intake valve. They have been estimated to 120° and 177° , however, these boundaries are not empirical and could be subject to change.

In order to achieve what Figure 17 and Figure 18 represent, the intake manifold must be designed correctly. Otherwise, the pressure wave will not arrive at the desired time, so it can become counterproductive. The intake manifold length for the D1 camshaft is shown in Figure 19 and in Table 2. The arrival of the pressure wave has been set to 150° , which is inside the boundaries estimated previously. The angle between the intake valve opening and the arrival of the pressure wave ($\Delta\theta$) is 163° . This parameter can vary depending on the desired arrival of the pressure wave. Longer angles will increase the manifold length.

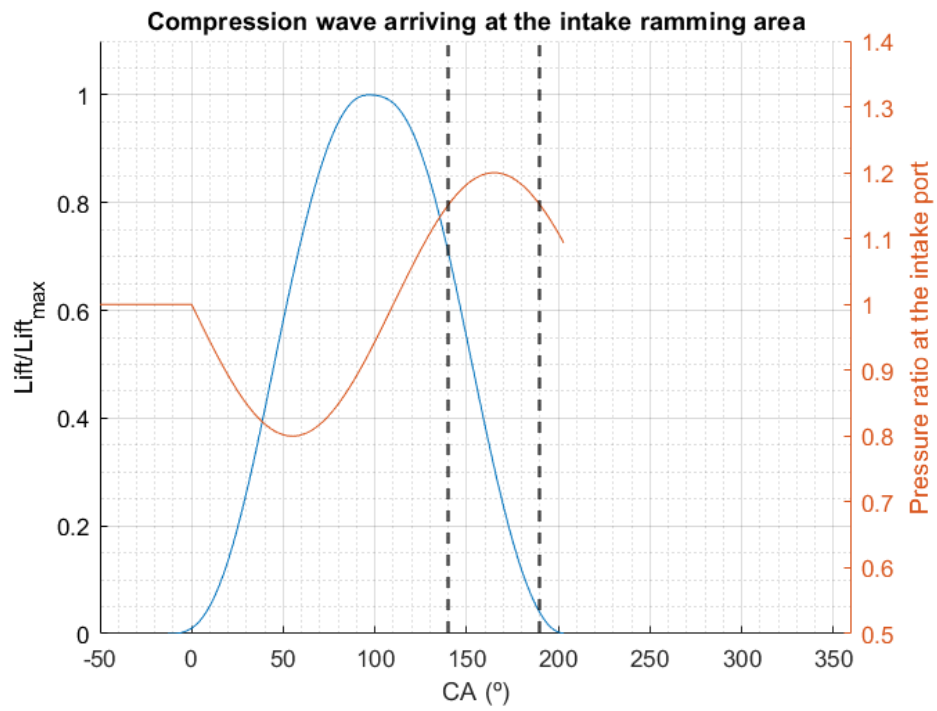


Figure 17. Ideal arrival of the pressure wave for D1 camshaft configuration.

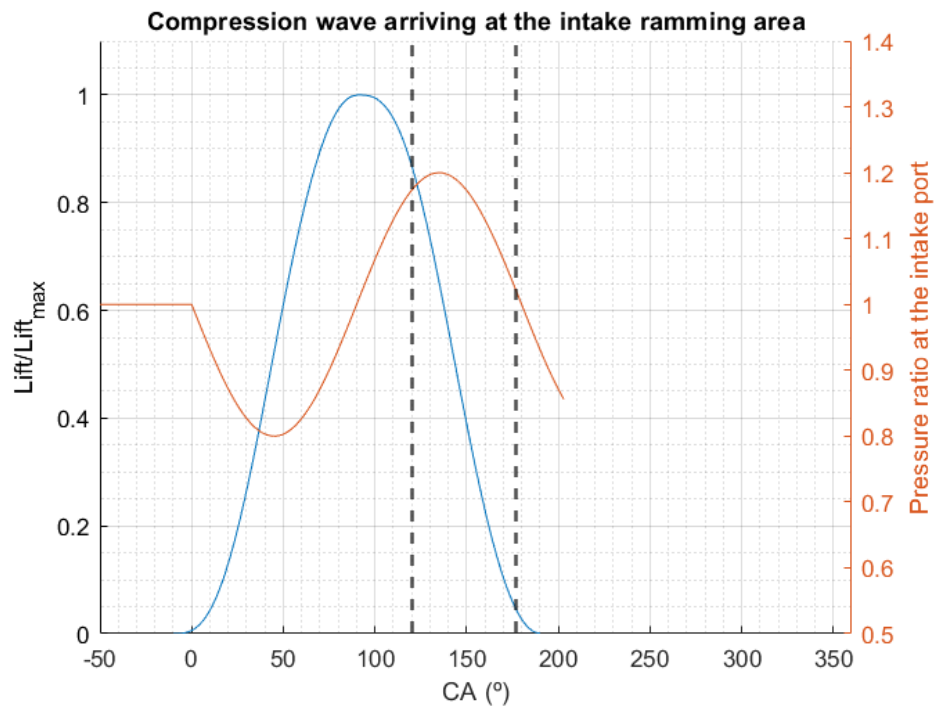


Figure 18. Ideal arrival of the pressure wave for s10 camshaft configuration.

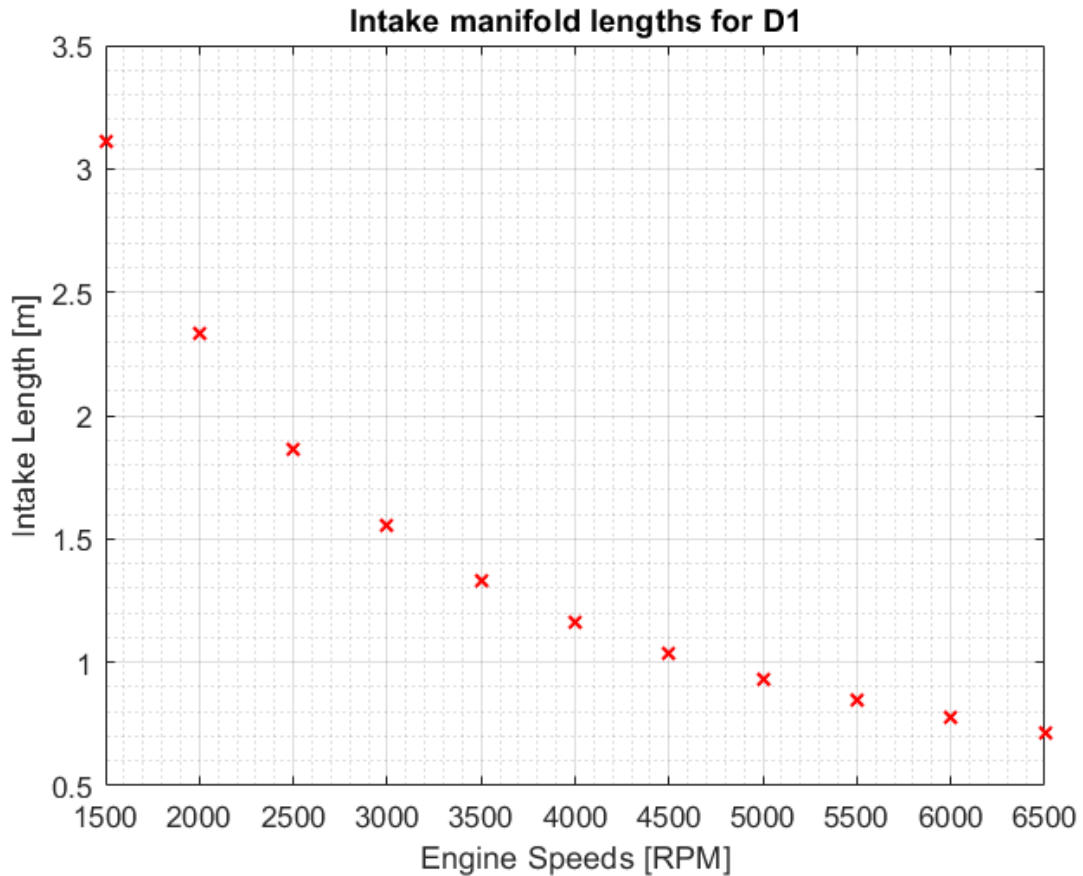


Figure 19. Intake manifold length for different engine speeds for the D1 camshaft configuration.

<i>Engine speed [RPM]</i>	2000	2500	3000	3500	4000
<i>Length [m]</i>	2.331	1.865	1.554	1.332	1.166
<i>Engine speed [RPM]</i>	4500	5000	5500	6000	6500
<i>Length [m]</i>	1.036	0.932	0.848	0.777	0.717

Table 2. Intake lengths from Figure 19.

The intake manifold lengths for lower engine speeds are excessive, as up to 3000 RPM the intake lengths are above 1.5 m. From 4500 to 6500 RPM, the length shortens to 1.036 m and 0.717 m respectively, which is acceptable. Even though the engine can reach those revolutions, it only runs up to 3750 RPM at the Shell EcoMarathon competition, thus, the length of the intake manifold should be within the 2500 - 4000 RPM range, which corresponds to 1.865 m and 1.165 m respectively.

The intake manifold length for the s10 camshaft valve timings is shown in Figure 20. The arrival of the pressure wave has been set to 135° , which is inside the range estimated. The angle between the intake valve opening and the arrival of the pressure wave is 145° , as it opens 3° later than the D1. The arrival of the pressure wave can be set this early due to the early closing of the intake valve, only 10° after BDC. The lengths obtained with the s10 camshaft and shown in Table 3

are shorter, as the duration has decreased. The comparison between both camshafts is shown in Figure 21.

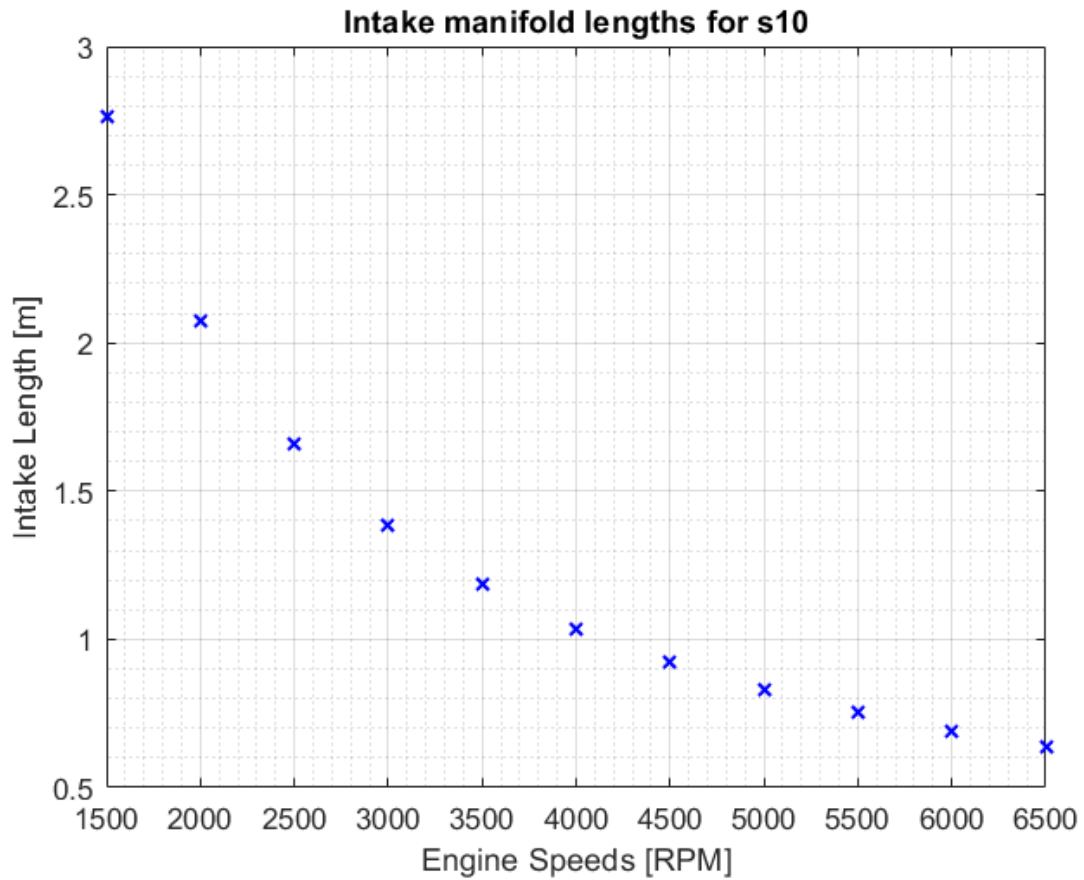


Figure 20. Intake manifold length for different engine speeds for the s10 camshaft configuration.

<i>Engine speed [RPM]</i>	2000	2500	3000	3500	4000
<i>Length [m]</i>	2.074	1.659	1.382	1.185	1.037
<i>Engine speed [RPM]</i>	4500	5000	5500	6000	6500
<i>Length [m]</i>	0.922	0.829	0.754	0.691	0.638

Table 3. Intake lengths from Figure 20.

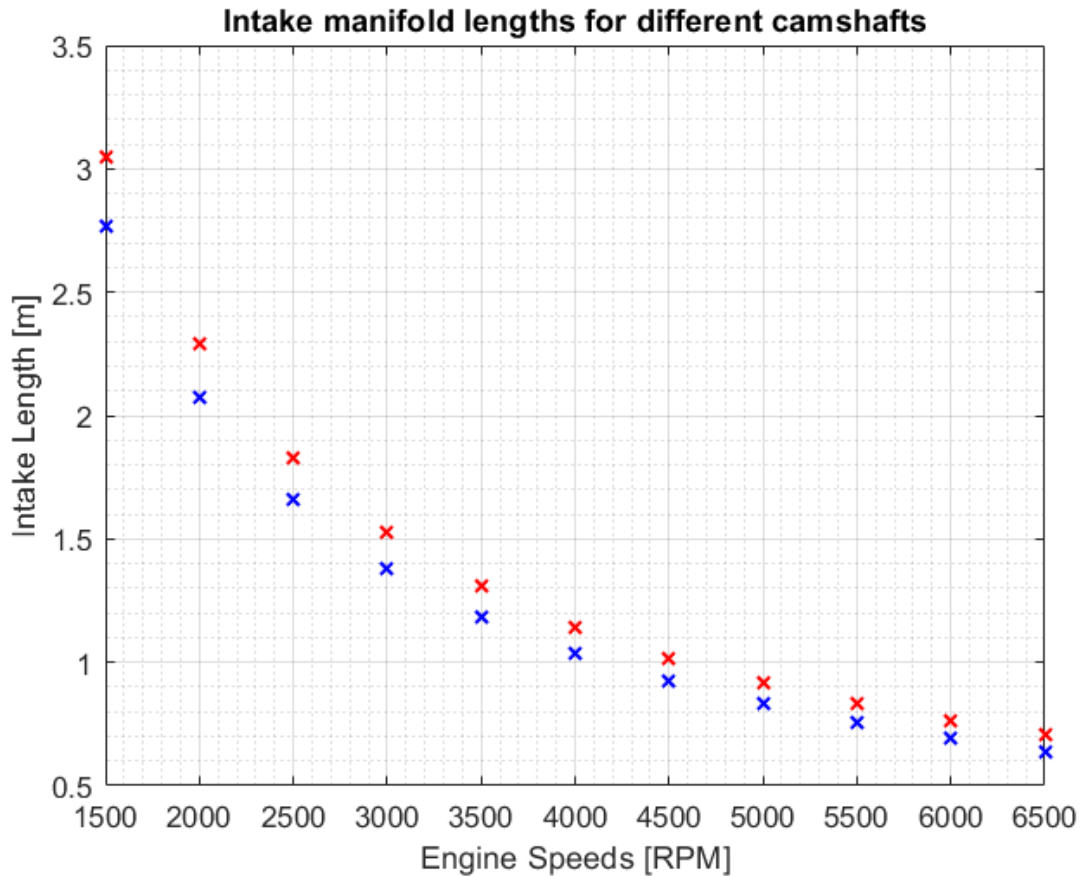


Figure 21. Intake manifold length for different engine speeds for the s10 and D1 camshaft configurations.

4.2 Sensibility analysis

As mentioned earlier in the Chapter, the intake length changes depending on the desired arrival of the pressure wave and the engine speed. If $\Delta\theta$ is increased, the intake manifold lengths for the D1 camshaft will increase, as shown in Table 4, whereas increasing the engine speed will decrease the intake manifold length.

For a late arrival of the pressure wave at low engine speeds, which corresponds to the third column, the intake manifold has to be extremely long, up to 3.68 m. It is not interesting to design the intake manifold length for those engine speeds due to the low flow velocities and excessive length of the manifold. For an arrival at 160°CA and 140°CA , the lengths are similar to those obtained in Chapter 4.1, as they are close. When the arrival is produced at 140°CA , the intake manifold length for mid engine speeds are acceptable, reducing in 6.16% the length with respect to the 150°CA arrival and 11.6% with respect to the 160°CA arrival at 3500 RPM.

If the duration is reduced even more, the lengths decrease accordingly, as shown in Figure 22. If the arrival is set at 100°CA , the range of lengths obtained are 2.155 m at 1500 RPM and

RPM \ $\Delta\theta$	140°	160°	180°
1500	2.917	3.299	3.68
2000	2.188	2.474	2.76
2500	1.75	1.979	2.208
3000	1.459	1.649	1.84
3500	1.25	1.414	1.577
4000	1.094	1.237	1.38
4500	0.972	1.1	1.227
5000	0.875	0.99	1.104
5500	0.796	0.9	1.003
6000	0.729	0.825	0.92
6500	0.673	0.761	0.849

Table 4. Manifold lengths for various engine speeds and pressure waves arrivals

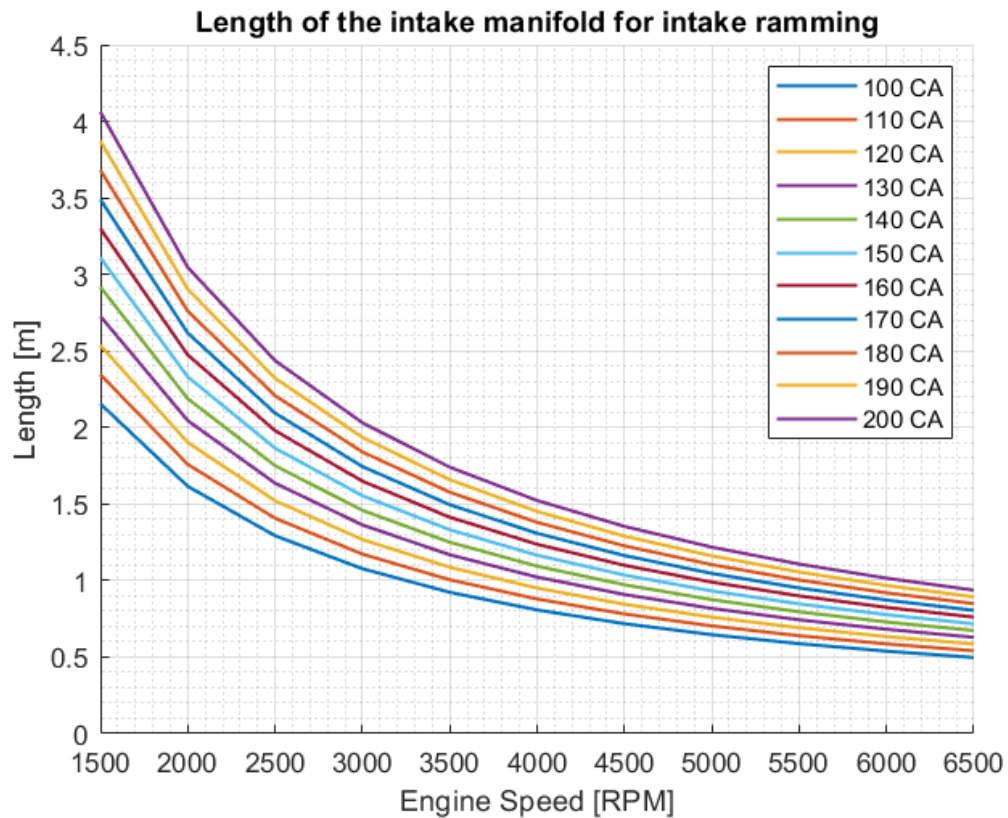


Figure 22. Intake manifold length for different engine speeds and valve timing configurations.

0.497 m at 6500 RPM, while at 3500 RPM the length is 0.923 m. This would be an early arrival of the pressure wave, so it could be detrimental. There is a compromise between the arrival of the pressure wave and the manifold length, as it is desirable to design an intake manifold as light as possible to maximize the power to weight ratio but without causing a premature arrival of the pressure wave. An early arrival of the pressure wave could cause the flow to choke, as the pressure of the cylinder could be higher than the pressure at the intake port. This has to be avoided by all means, as that would definitely lead to a decrease in the volumetric efficiency.

5 Conclusions

5.1 Methodology conclusions

The calculations performed throughout this project are theory based, but they should have been sustained by empirical data, as an specific engine wants to be tested. The references used for this project provide useful information and guidelines on how to take advantage of intake ramming, but it is difficult to proceed without testing. Nevertheless, the study of the pressure waves and the procedure to calculate the estimated length of the manifold to produce intake ramming provides a good estimation of what happens in the duct and what parameters affect the intake ramming.

It would have been more precise to test different lengths of the intake manifold at the test rig of the Ecocar engine and compare the performance of each pipe as well as the coherence between the theoretical and practical results. Kistler, a swiss manufacturer of measuring devices and sensors, provided a pressure sensor to perform the measurements, but it was not possible to install it at the engine head due to lockdown. The pressure sensor is shown in Figure 23.

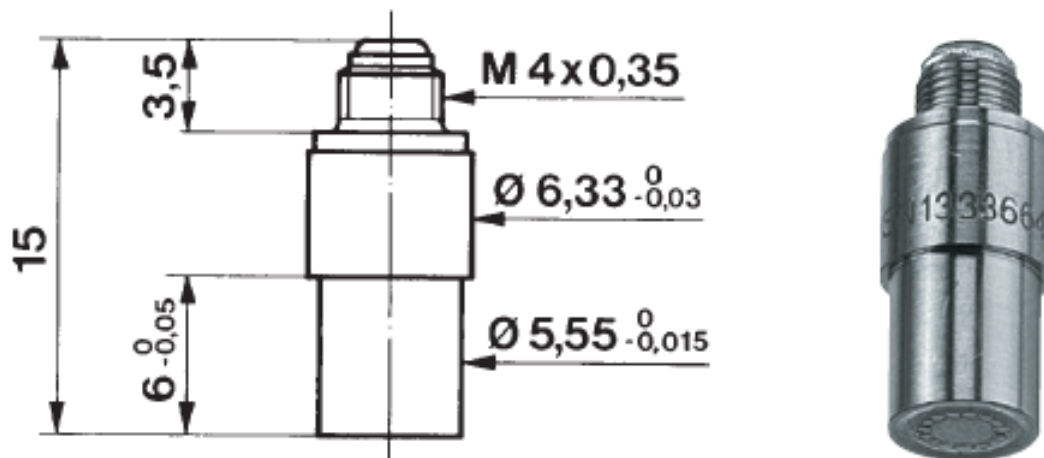


Figure 23. Kistler sensor type 601A [9].

5.2 Results conclusions

The resulting length of the manifold is often overly long, as at the Shell EcoMarathon the engine runs at 3750 RPM at maximum. Higher engine speeds would decrease the length of the manifold and increase the volumetric efficiency. The problem with running at low engine speeds is that the low velocities involved reduce the impact of the pressure waves in pressure charging, therefore, it

is important to investigate if it is worth it to add extra weight in exchange of better performance. If the power to weight ratio is decreased when a larger intake manifold is added, it will not be worth it.

Different camshafts have been tested at various engine speeds, resulting in diverse intake manifold lengths. The most interesting lengths are those obtained at 3500-4000 RPM, which is the maximum engine speed when competing and also the shorter ducts with respect to those obtained at lower engine speeds. Depending on the arrival of the pressure wave, the ducts length are estimated to be from 1.1 m to 1.5 m approximately, which is still long for an intake runner.

For this matter, the better solution would be to design a helical runner instead of the classic straight pipe, as the latter would be completely oversized when compared to the engine. An example of this has been studied in [10], where an helical runner was designed and tested. It is shown in Figure 24. The helical runner enables the possibility to pressure charge the Ecocar engine, as two turns with a diameter D of 0.19 m and a rise H equal to the diameter would be enough to cover 1.25 m, as the length L of the helix is:

$$L = \sqrt{H^2 + (\pi \cdot D)^2}$$

In [11], it is proposed to manufacture the runner in ABS P400 by additive manufacturing, which could be interesting in terms of weight saving when compared to cast iron and more complex shapes can be obtained, such as the helix. In addition, the intake manifold does not have to withstand the high temperatures produced at the exhaust stroke, even though some gasses recirculate due to the overlap period between exhaust and intake stroke, so the ABS could be used as there would not be risk of heat deflection nor losses of mechanical properties.

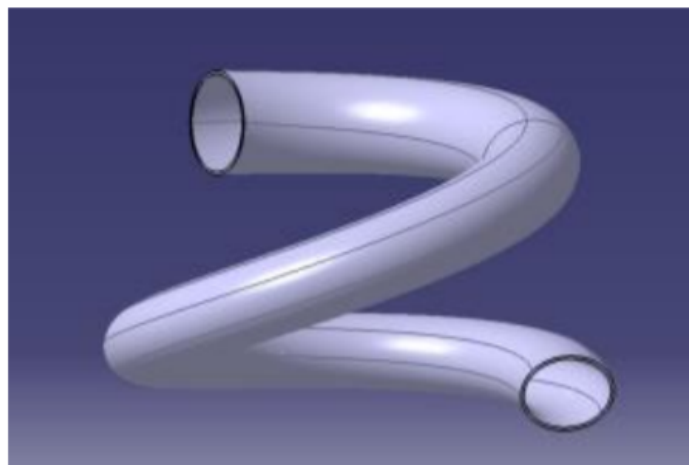


Figure 24. Helical runner.

5.3 Recommendations for future research

Once the test rig is available, it would be interesting to analyze the pressure waves of the actual intake duct with the pressure sensor provided by Kistler. It is important to note that the sensor is piezoelectric, so it will measure the changes in pressure at the intake pipe precisely. It is recommended to drill at the engine head in order to obtain the pressure change at the intake port; drilling in the pipe is not recommended due to the fact that one hole needs to be made per pipe and the pressure measurements from the sensor would not be those of the intake port.

After that, it would be desirable to vary the length of the runner and check the performance of the lengths purposed in this project in order to analyze whether or not the theory applies to the Ecocar engine. The test rig at DTU was configured to measure brake power and torque, therefore, it only requires the manufacture of the pipes to check the performance of each length. Maybe a prior simulation with a computer program designed for acoustic charging, Ricardo WAVE for instance, could lead to results without manufacturing various intake manifold lengths.

As mentioned in Chapter 5.2, the proposed lengths for the intake manifold are maybe too long to be implemented. A solution could be the design of an helical runner manufactured by additive manufacturing. This represents an improvement with respect to cast iron, as it is lighter and more complex shapes can be made. In addition, the helical runner would produce a better mixing with the fuel due to the swirl. However, the ABS P400 is far more expensive than cast iron, as the first costs 70 EUR/kg approximately while the second costs roughly 1.4 EUR/kg. This will be developed in Chapter 6.

Regarding the valve timing, even though the D1 camshaft has proven to be more efficient and provide higher torque, as Figure 25 shows, it would be interesting to test s10 camshaft with a intake manifold length that improves the pressure charging effect, as it needs shorter intake manifolds than the D1 due to its shorter duration of the intake valve.

Any attempt of investigating the pressure waves at the exhaust has been dismissed due to the fact that in 4 stroke engines the effect of pressure waves for scavenging is limited, according to [3]. It has some influence on performance at high speeds, which can not be reached by the Ecocar engine.

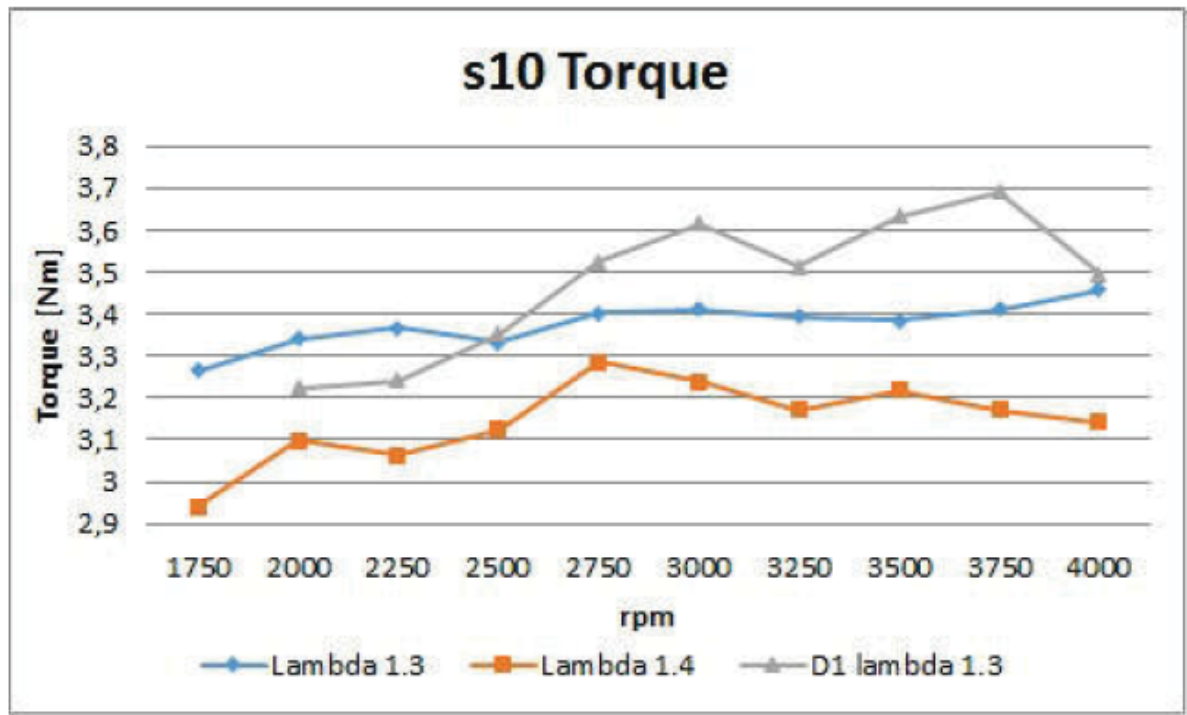


Figure 25. Torque of the s10 (blue and orange) and D1 (grey) camshafts by [8].

6 Economic assessment

Throughout this section, the costs and savings associated to the manufacture of an intake manifold that improves the performance and fuel efficiency will be analyzed.

The costs manufacturing various intake manifolds can be diverse, as it depends on the amount of pipes manufactured for the investigation, their length and the material used for their construction. The materials that will be taken into account will be cast iron for straight pipes and ABS P400 for the helix made by additive manufacturing. The costs per kilogram of material are shown in Table 5.

	Cast iron	ABS P400
Price	1.39 €/kg [13]	70 €/kg [14]
Density	7300 kg/m ³	1070 kg/m ³ [15]

Table 5. Cast iron and ABS prices and densities.

Even though the density of the ABS is a tenth of the density of the cast iron, the cost per kilogram is fifty times greater. The intake manifold runner does not withstand any force other than its own weight, the weight of the air filter and the vibrations generated when the engine is running, so the ABS could be a interesting choice from the performance standpoint but it is worse from the economic point of view. If the pipes are assumed to be designed with an outer diameter of 45 mm and inner diameter of 30 mm, the section of the runner can be obtained. Then, the cost per meter of pipe can be easily achieved by multiplying the density and price per kilogram, as follows:

$$A_t = \frac{\pi \cdot (45^2 - 30^2)}{4} = 550 \text{ mm} = 5.5e - 4 \text{ m}^2$$

- Cast iron:

$$1.39 \cdot 7300 \cdot A_t \cdot \frac{\text{EUR}}{\text{kg}} \cdot \frac{\text{kg}}{\text{m}^3} \cdot \text{m}^2 = 5.578 \text{ EUR/m}$$

- ABS P400:

$$70 \cdot 1070 \cdot A_t \cdot \frac{\text{EUR}}{\text{kg}} \cdot \frac{\text{kg}}{\text{m}^3} \cdot \text{m}^2 = 41.17 \text{ EUR/m}$$

The cost per meter is significantly greater for the ABS compared to the cast iron. However, the simplicity of the additive manufacturing and the capability of producing complex shapes without casting and machining iron is interesting. Maybe a solution could be to simulate with a computer program, such as Ricardo WAVE, the performance of the engine with different intake manifold lengths prior to the manufacturing of the runners.

Regarding the fuel consumption of the Ecocar, the intake pressure charging improves the brake power of the engine as it increases the volumetric efficiency, therefore, the brake specific fuel consumption decreases, which means less fuel consumption with respect to brake power. The price of Ethanol in Sweden at 12th August 2020 is 1.25 €per liter, which was the price of the closest country from Denmark found in [16]. Table 6 shows the amount saved for different efficiency improvements. The savings are not relevant, as the Ecocar engine testing and the ShellEcoMarathon competition do not require excessive amounts of fuel.

Efficiency increment	EUR per liter saved
0.5%	0.00625
1%	0.0125
1.5%	0.01875
3%	0.0375

Table 6. Savings in fuel due to improved efficiencies

References

- [1] Piltan, F., Sulaiman, N. (2011). Control of IC Engine: Design a Novel MIMO Fuzzy Backstepping Adaptive Based Fuzzy Estimator Variable Structure Control, *International Journal of Robotics and Automation*, 2(5), 360-380.
- [2] Retrieved from: <https://makinandovelez.wordpress.com/2017/11/12/diagrama-pv-de-un-motor-de-ciclo-teorico-otto/>
- [3] Sorenson, S. C. (2017). Internal Combustion Engine Principles with Vehicle Applications. *DTU Mekanik*.
- [4] Gordon P. Blair (1999). Design and Simulation of Four-Stroke Engines, *SAE International*.
- [5] Prado. D (2019, February 19) Qué es el VTEC de Honda y cómo funciona. Retrieved from: <https://gascommunity.com/que-es-el-vtec-de-honda-y-como-funciona/>
- [6] Volkswagen (2016), The 2.0l FSI engine with 4-valve technology Retrieved from: <https://docplayer.net/20911419-The-2-0l-fsi-engine-with-4-valve-technology.html>
- [7] Hadjkacem, S., Ali, M., Salah, M.(2018). Volumetric Efficiency Optimization of Manifold with Variable Geometry Using Acoustic Vibration for Intake Manifold with Variable Geometry in Case of LPG-Enriched Hydrogen Engine, *Arabian Journal for Science and Engineering*.
- [8] M. Thage and G. Singh (2015). Analysis and optimization of the ecocar IC engine, *DTU Mekanik*.
- [9] Kistler. Retrieved from: <https://intertechnology.com/Kistler/pdfs/Pressure-Model-601A-601H.pdf>
- [10] S. Ravi, B. Rahul, E. Shibin, and V. Vijay (2018). Design and Simulation of Helical Intake Manifold, *IJRESM*, 1(10).
- [11] M. Aiamunoori, S. Kumar, and Y. Ravi (2017). Design and manufacturing of spiral intake manifold to improve volumetric efficiency of injection diesel engine by AM process, *Materials Today: Proceedings*,4.
- [12] F. Judistra, S. Friborg. (2019) Karakterisering af ny ethanoldrevet motor til DTU's økobil 2019.
- [13] Retrieved from: <http://www.iron-foundry.com/cast-iron-price-lb.html>
- [14] Retrieved from: <http://shopping.na3.netsuite.com/s.nl/c.635262/sc.2/category.1923/f>

- [15] Retrieved from: <https://www.britannica.com/science/acrylonitrile-butadiene-styrene-copolymer>
- [16] Retrieved from: <https://www.globalpetrolprices.com/ethanol-prices/>
- [17] United Nations. Retrieved from: <https://www.un.org/sustainabledevelopment/sustainable-development-goals/>
- [18] Durán, M. R. (2020 June 23). Retrieved from: <https://commons.wikimedia.org/wiki/File:Averager-fleet-CO2-emissions-Norway.png>

7 Appendix A: Sustainable Development Goals

The Sustainable Development Goals consist of 17 goals adopted by the UN Member States in 2015. The goals aim to improve the situation of the planet by respecting its limits, end with the poverty and increase the wellness of the people. In order to do so, the world leaders called at SDG summit in 2019 the Decade of Action, to encourage people to be involved in the achievement of the goals and call for the action, as it is planned to fulfill the goals before 2030.

Among the objectives set by the UN, there are several covered by this project: the Sustainable Development Goal number 7 'Energy', number 9 'Infrastructure, industrialization' and number 12 'Sustainable consumption and production', they all mention efficiency as the mindset that industry and consumers must have in order to achieve the objectives set for 2030. Just as Goal number 12 declares: 'Sustainable consumption and production is about doing more and better with less. It is also about decoupling economic growth from environmental degradation, increasing resource efficiency and promoting sustainable lifestyles'[17]. The increase of efficiency in internal combustion engines and the reduction of pollutants by EU measures such as the European Emission Standards has improved the quality of the air at the cities, thus, the health of its people. For instance, Norway has reduced dramatically CO₂ emissions for new passenger cars, as Figure 26 shows.

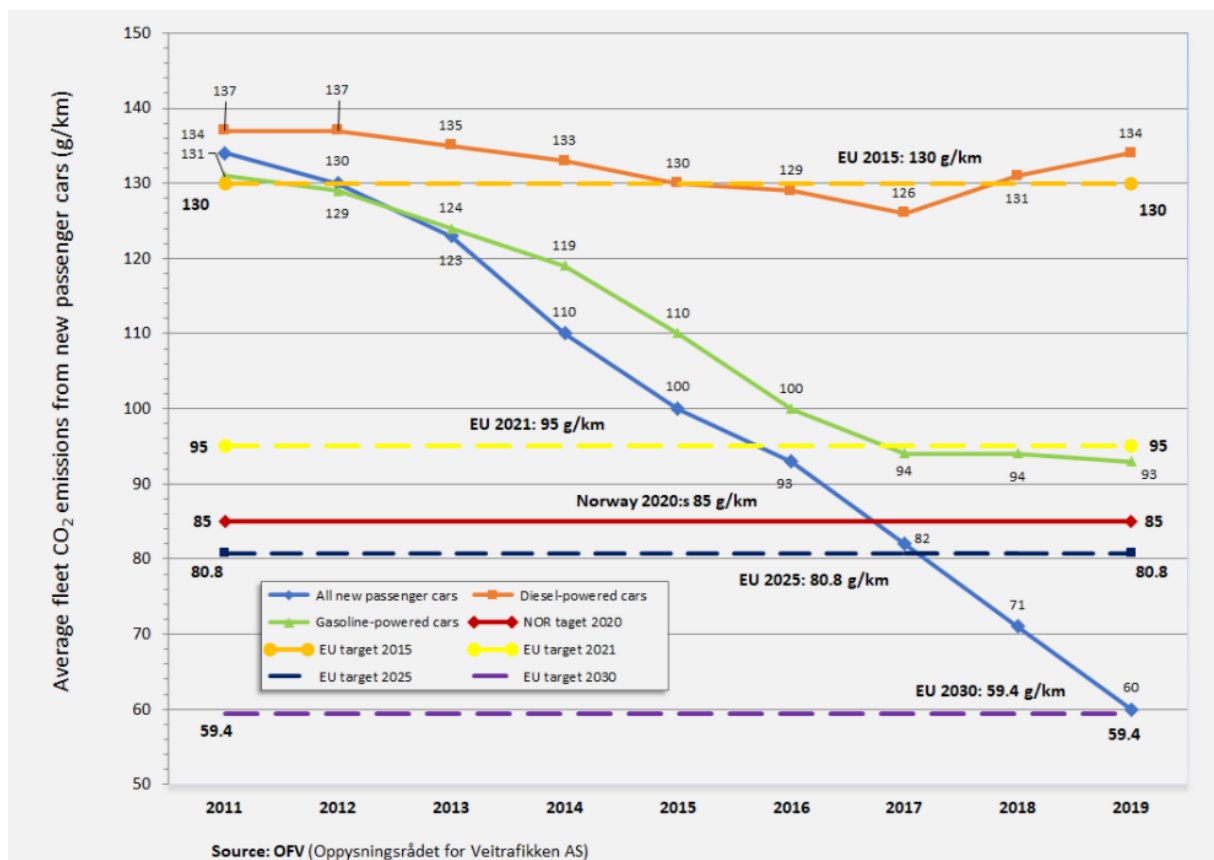


Figure 26. Norway average fleet CO₂ emissions for new passenger cars [18].

The electrification of the transportation is taking over the internal combustion engines step by step, but at the moment, the world depends on fuel. It is therefore crucial to improve and maximize the efficiency of these engines with new inventions and research, so emissions and pollutants are reduced or even eliminated.